



HAL
open science

Multiple scale bifurcation analysis for finite-dimensional autonomous systems

Angelo Luongo, Angelo Di Egidio, Achille Paolone

► **To cite this version:**

Angelo Luongo, Angelo Di Egidio, Achille Paolone. Multiple scale bifurcation analysis for finite-dimensional autonomous systems. *Recent Research Developments in Sound and Vibration*, 2002, 1, pp.161-201. hal-00812537

HAL Id: hal-00812537

<https://hal.science/hal-00812537>

Submitted on 12 Apr 2013

HAL is a multi-disciplinary open access archive for the deposit and dissemination of scientific research documents, whether they are published or not. The documents may come from teaching and research institutions in France or abroad, or from public or private research centers.

L'archive ouverte pluridisciplinaire **HAL**, est destinée au dépôt et à la diffusion de documents scientifiques de niveau recherche, publiés ou non, émanant des établissements d'enseignement et de recherche français ou étrangers, des laboratoires publics ou privés.

Multiple scale bifurcation analysis for finite-dimensional autonomous systems

Angelo Luongo¹, Angelo Di Egidio¹ and Achille Paolone²

¹Dipartimento di Ingegneria delle Strutture, Acque e Terreno, University of L'Aquila, Monteluco di Roio, 67040 L'Aquila, Italy; ²Dipartimento di Ingegneria Strutturale e Geotecnica, University of Rome "La Sapienza", via Eudossiana, 18, 00184 Roma, Italy

Abstract

Codimension- M bifurcations for general, finite-dimensional, autonomous, nonlinear dynamical systems are analyzed. Basic concepts of bifurcation analysis are first summarized. Some sample structures are then introduced as prototype systems for low-codimension bifurcations. Mechanical as well as geometrical aspects of the bifurcation phenomenon are discussed. Eigensolution Sensitivity Analysis is then illustrated for Jacobian matrices admitting complete (non-defective) or incomplete (defective) systems of eigenvectors. The use of integer and fractional power series of a perturbation parameter is discussed and a reconstitution procedure for eigenvalue sensitivity equations is suggested. The Multiple Scale Method of analyzing multiple bifurcations is then illustrated. Non-

defective bifurcations are first considered under general conditions of resonance among the critical eigenvalues. The structure of the Amplitude Modulation Equations at various orders of the perturbation procedure is obtained and several algorithmic aspects discussed, namely: the search for steady-state solutions, expansion vs ordering of the bifurcation parameters, reconstitution of the Amplitude Equations and imperfections accounting. Defective bifurcations are then analyzed by exploiting a formal analogy with Sensitivity Analysis. By limiting the study to bifurcation points at which the Jacobian matrix contains a unique critical Jordan block, the cases of defective divergence and defective Hopf bifurcations are analyzed. In both cases the reconstitution procedure is applied and the structure of the relevant bifurcation equations is given. In particular, rules to obtain the equations at any order of approximation are furnished. The techniques illustrated are finally employed to study several low-codimension bifurcations. In particular, the post-critical behavior of the prototype systems previously introduced is analyzed and some results commented.

1. Introduction

Nonlinear autonomous dynamical systems, when subjected to quasi-static variations of the control parameters, can visit a set of equilibrium positions, named *fundamental path*. It is possible that, for a critical combination of such parameters, a sudden qualitative modification of the local phase-portrait will manifest itself. This circumstance occurs when at least one eigenvalue of the Jacobian matrix crosses the imaginary axis, thus entailing the loss of stability of the fundamental path. In this case a *bifurcation* is said to occur. The Local Bifurcation Theory [1,2] aims to furnish a complete description of the system's behavior in the parameter space around the bifurcation point.

Analytical techniques have been developed [2,3] to reduce the N -dimensional original system to an M -dimensional system, with $M \ll N$, able to capture all the essential qualitative aspects of the bifurcation phenomenon. The most popular method is the Center Manifold Method [2], which has been extensively employed to solve a large variety of bifurcation problems. It consists in (a) describing the manifold on which the postcritical dynamics develop (often by solving a functional equation by series) and (b) transforming the relevant bifurcation equations into the simplest form, by using the Normal Form Theory [1-4]. Low-codimension bifurcations have been studied by this method. Very often, however, attention has been focused on the *classification* of these bifurcations in terms of general (unfolding) parameters, rather than on the solution of practical problems in terms of the original physical parameters. Moreover, consistently with this approach, explicit expressions of the coefficients of the reduced bifurcation equations in terms of the derivatives of the original vector field, do not seem to be available, so that the procedure has to be repeated for each specific problem.

However, a more engineering-oriented approach to the problem was developed in the sixties, particularly in the U.K. [5-8], in the framework of the theory of elastic stability (buckling), known as the Theory of Static Perturbation. This approach consists in expanding in series of a perturbation parameter both the state variables and the parameters (usually only one in the original works, even for multiple static bifurcations) to obtain a set of perturbation equations to be solved in sequence. At each step of the procedure, solvability conditions (Freedholm alternative) [9] furnish the link between the state variables and the parameter, thus describing asymptotically the bifurcated equilibrium

paths. The method thus makes it possible to avoid a preliminary description of the center manifold which, in contrast, is obtained at the end of the procedure, if desired.

Obviously the Theory of Static Perturbation works well only if the bifurcation is of a static type, i.e. if the critical eigenvalues have no imaginary parts: if they do, dynamic aspects must be accounted for. The simplest case of dynamic bifurcation (only a couple of complex critical eigenvalues) was solved by Hopf, using an adapted Lindsted-Poincaré method [10], in which not only the unknown frequencies was expanded in series, but also the parameter. The structure of the algorithm appears very close to that of the static perturbation, since the suppression of the so-called secular terms is equivalent to the Fredholm alternative, if the space of the operator is that of periodic functions.

The static perturbation method and the Lindsted-Poincaré method, however, do not furnish any bifurcation equation, but only the steady-solutions (equilibria or periodic motions, respectively). In contrast, Nayfeh [11] and Smith and Morino [12] presented an application of the Multiple Scale Method [10] to a flutter problem, by obtaining a bifurcation equation in the amplitude of the critical mode governing the asymptotic dynamics. A generalizations of the method to study codimension-1 bifurcation problems for multi-dimensional autonomous and non-autonomous systems can be found in [13,14]. Other applications of the method have subsequently been presented in [15-22]. More recently the method has been applied to solve more complex bifurcations including resonances [23-27]. In particular, the expression of the coefficients of the bifurcation equations in terms of the original vector field has been obtained.

In this paper a systematic Multiple Scale approach to the problem is illustrated. After a brief summary of the basic concepts of bifurcation analysis (Sect. 2) some elementary mechanical systems are qualitatively analyzed to illustrate phenomenological aspects (Sect. 3) (readers already acquainted with Dynamical System Theory can skip Sect. 2 and go directly to Sect. 3). A sensitivity eigenvalue analysis is then performed in order to introduce concepts useful for nonlinear bifurcation analysis (Sect. 4). The Multiple Scale method is illustrated in Sect. 5 for non-defective systems and in Sect. 6 for a class of defective systems, given that no comprehensive treatment of them is yet available. Finally several examples and results are presented in Sect. 7, and some conclusions drawn in Sect. 8.

The paper is mainly based on results obtained by the authours in previous works. However, the whole matter has been reorganized in a more homogeneous manner and some new procedures (Sect. 6) are also presented. Further details (e.g. the explicit expressions of the coefficients of the bifurcation equations, not given here) can be found in the original papers.

2. Basic concepts of bifurcation analysis

Some fundamental elements of bifurcation analysis are recalled [1-4]. In particular the concepts of codimension, imperfections and linear codimension are discussed to provide a background for further developments.

2.1. Bifurcation points

The free evolution of a finite-dimensional dynamical system is governed by a

parameterized vector field of ordinary differential equations:

$$\dot{\mathbf{y}} = \mathbf{G}(\mathbf{y}, \boldsymbol{\mu}) \quad \mathbf{y} \in \mathbb{R}^N \quad \boldsymbol{\mu} \in \mathbb{R}^P \quad (1)$$

where \mathbf{y} is the *state-variable vector*, $\boldsymbol{\mu}$ the control parameter vector and the dot denotes time-differentiation. The set of solutions to Eq. (1) $\boldsymbol{\phi}(\mathbf{y}, t; \mathbf{y}(\mathbf{0}))$ is called the (parameter-dependent) *flow* of the vector field.

A point $(\mathbf{y}_E, \boldsymbol{\mu}_E)$ is an equilibrium (or fixed) point if $\mathbf{G}(\mathbf{y}_E, \boldsymbol{\mu}_E) = \mathbf{0}$. It is *hyperbolic* if the Jacobian \mathbf{G}_y^E evaluated at $(\mathbf{y}_E, \boldsymbol{\mu}_E)$ admits all eigenvalues λ_k with non-zero real part; it is *non-hyperbolic* if at least one eigenvalue lies on the imaginary axis. Hyperbolic equilibrium points are stable if $\text{Re}(\lambda_k) < 0 \forall k$, and unstable if $\text{Re}(\lambda_k) > 0$ for at least one k . The stability of non-hyperbolic points, in contrast, depends on the higher-order derivatives of \mathbf{G} .

Hyperbolic equilibrium points are said to be *structurally stable*, since slight variations of $\boldsymbol{\mu}$ do not qualitatively alter the flow around the point. In contrast, if a non-hyperbolic point is perturbed, a sudden qualitative modification manifests itself. For example, new equilibrium points or time-dependent solutions such as periodic, quasi-periodic or even chaotic motions can be created (or destroyed) by perturbations. Non-hyperbolic points are therefore known as *critical*, *singular* or *bifurcation* points. The purpose of Local Bifurcation Theory is to analyze the nature of the flow near the bifurcation points when the parameters are varied. No attention is paid instead to the study of the hyperbolic points, since the qualitative local dynamics does not depend on the parameters.

It follows from the Center Manifold Theorem [1-4] that a system that is topologically equivalent to Eq. (1) exists and is able to capture its qualitative dynamics around a bifurcation point. It consist of a small set of *bifurcation equations*, equal in number to the dimension of the critical eigenspace of \mathbf{G}_y^0 (i.e. to the number of its eigenvalues having zero real parts). An effective procedure to obtain such bifurcation equations is illustrated below.

2.2. Codimension

An important question arises about the dimensions of the parameter subspace in which *all the possible qualitative dynamics* occurring near a bifurcation point appear. The problem is addressed as follows. In order for a particular bifurcation to occur, some constraints among the parameters must be satisfied, so that bifurcation points lies on some manifolds \mathcal{M} of the parameter space \mathcal{P} . If C is the number of constraints characterizing the bifurcation, then \mathcal{M} has codimension- C , i.e. C is the smallest dimension of a manifold \mathcal{C} which transversally intersects \mathcal{M} . The more degenerated the bifurcation (i.e. the higher the number of constraints) the higher the codimension of \mathcal{M} . Thus a codimension- C manifold \mathcal{M} contains other bifurcations of higher codimension.

It would appear that a specific bifurcation point B of \mathcal{M} represents a *rare singularity* that could easily be removed by small perturbations of the parameters, rendering it unimportant to study. In contrast, if the system at B is embedded in a *family of systems* represented by a manifold \mathcal{C} that is transversal to \mathcal{M} , the *bifurcation naturally appears* on \mathcal{C} . Moreover, any perturbation modifying \mathcal{C} to another transversal manifold \mathcal{C}' , changes

the bifurcation point to B' , but cannot destroy the bifurcation. Bifurcations of codimension- C cannot therefore be avoided if a family of C parameters is considered. The idea underlying parameterization is that, by using families rather than single vector fields, it is possible to regain a persistent (i.e. *robust*) behavior, notwithstanding the structural instability of the vector field. The C parameters of the family will be referred to as *bifurcation parameters*.

The parameterized family of systems containing all possible qualitative behavior near the bifurcation is called the *unfolding* of the bifurcation; if the number of parameters is minimal, i.e. equal to the codimension, then it is called a *universal unfolding*.

Some examples are now given. In a one-parameter one-dimensional vector field $\dot{y} = g(y, \mu)$, $y \in \mathbb{R}$, $\mu \in \mathbb{R}$, $g(0,0) = 0$, a bifurcation occurs at $(0, 0)$ when the following conditions are satisfied (index denotes differentiation and apex evaluation at the point): (a) a saddle-node bifurcation (limit or turning point) when $g_y^0 = 0$; (b) a transcritical bifurcation when $g_y^0 = 0$, $g_\mu^0 = 0$; (c) a pitchfork bifurcation when $g_y^0 = 0$, $g_{yy}^0 = 0$, $g_\mu^0 = 0$, the higher-order derivatives being in all cases different from zero. Therefore, the bifurcations are of codimension C equal to 1, 2 and 3, respectively. In a one-parameter family, only the saddle-node bifurcation is structurally stable, the other two appearing naturally only in a two- or three-dimensional parameter space, respectively, in which they must be embedded.

2.3 Imperfections

The codimension of a bifurcation naturally depends on the properties assumed for the system. For example, if symmetry properties or fixed values for several physical constants are admitted (perfect system), a codimension C' is found for a singular vector field B in a space of parameters \mathcal{P}' . However, it may be that, in a space $\mathcal{P} \supset \mathcal{P}'$ in which small asymmetries and small deviations from the nominal values of the constants are accounted for, the codimension of B is $C > C'$, so that the parameterized family is structurally stable in \mathcal{P}' but not in \mathcal{P} . In this case, the reduced model must be judged inadequate, and a larger universal unfolding must be considered. The additional $C - C'$ parameters to be taken into account are usually called *imperfections*. They describe qualitatively new dynamics with respect to *ideal perfect systems* belonging to \mathcal{P}' . Terms such *perfect bifurcation* (in \mathcal{P}') and *imperfect bifurcation* (in \mathcal{P}) are also occasionally used. For example, if a fork bifurcation is considered in the space of perfect symmetric systems, it has a lower codimension, since the condition $g_{yy}^0 = 0$ is *a priori* satisfied in that space. If asymmetries are reintroduced, the codimension becomes 3, the asymmetries being considered as imperfections. It should be noted that the notion of imperfection is not an absolute concept, but is rather relative to the model which has conventionally, for physical reasons, been assumed to be perfect.

2.4 Fundamental path

Among the properties postulated for the ideal, perfect system, it is of particular interest to admit the existence of a *known equilibrium path* $\Gamma = \{(y_E, \mu_E) \mid \mathbf{G}(y_E, \mu_E) = 0\}$ (usually referred to as a fundamental path) for any μ close to its

bifurcation value μ_0 . This assumption means that: (a) no limit points exist along Γ ; (b) transcritical bifurcations are structurally stable in one-parameter families; (c) pitchfork bifurcations are structurally stable in: (i) two-parameter families of *non-symmetric* systems and (ii) in one-parameter families of *symmetric* systems. For such perfect systems, *additional parameters destroying the path Γ (and possibly leading to a limit point) are imperfection parameters.*

The existence of the fundamental path, $y_E = y_E(\mu)$, makes it possible to rewrite Eqs. (1) in the so-called local form [14,28]:

$$\dot{\mathbf{x}} = \mathbf{F}(\mathbf{x}, \mu) \quad \mathbf{x} \in \mathbb{R}^N \quad \mu \in \mathbb{R}^p \quad (2)$$

where $\mathbf{x} := \mathbf{y} - \mathbf{y}_E(\mu)$ are new state variables (often called *sliding coordinates*) and $\mathbf{F}(\mathbf{x}, \mu) := \mathbf{G}(\mathbf{y}_E(\mu) + \mathbf{x}, \mu)$ ⁽⁸⁾.

2.5. Linear codimension

The following remarkable property holds: *the constraint conditions defining a bifurcation from a known equilibrium path reduce to the degeneracy conditions of the eigenvalues of \mathbf{G}_y^0 , if generic non-vanishing nonlinearities are considered.* We define this constraint number M as the *linear codimension* of the bifurcation; it is the codimension of the manifold $\mathcal{M}_L \subseteq \mathcal{M}$, where all the eigenvalue degeneracy conditions are simultaneously satisfied. Due to the coincidence $C \equiv M$, the term ‘codimension’ will be used as an abbreviation for ‘linear codimension’ throughout the paper.

The degeneracy conditions are of the following two types: (a) conditions of non-hyperbolicity of the equilibrium point, of the types $\lambda_k = 0$ or $\text{Re} \lambda_j = 0$; (b) conditions of resonance among the critical frequencies $\omega_j := \text{Im} \lambda_j$, of the type $\sum_j k_{ij} \omega_j = 0$, $k_{ij} \in \mathbb{Z}$. Some examples are given in Fig. 1. Figures 1a and 1b show the critical eigenvalues (and their velocities) in codimension-1 bifurcations: the *divergence* ($\lambda_0 = 0$) and the *Hopf* ($\text{Re} \lambda_1 = 0$) bifurcations, respectively. Figures 1c, 1d and 1e show codimension-2 bifurcations: the *double-zero* ($\lambda_1 = \lambda_2 = 0$), the *Hopf-divergence* ($\lambda_0 = 0$, $\text{Re} \lambda_1 = 0$) and the *double-Hopf* ($\text{Re} \lambda_1 = \text{Re} \lambda_2 = 0$), respectively. When more than one Hopf bifurcation manifest themselves simultaneously, possible resonance conditions must be taken into account. These occur when the critical frequencies ω_j are linearly dependent. Thus, the double-Hopf bifurcation in Fig. 1e is nonresonant (of codimension-2) if ω_1 and ω_2 are in an irrational ratio, and it is resonant if $\omega_1 = n \omega_2$, with $n = 1, 2, 3, \dots$.

To sum up, the codimension of a bifurcation is equal to the number of critical eigenvalues (counting the complex conjugate ones in pairs) plus the number of (possible) resonance conditions among the critical frequencies.

One important property is linked to the codimension M : among bifurcation equations, only M describe the essential dynamics, such as stability and type of attractor, the remaining equations governing complementary aspects, such as phase-modulations.

⁽⁸⁾ Indeed, there is no strict need to build up the new function \mathbf{F} , since, as will become clearer below, the asymptotic analysis only requires knowledge of the derivatives of \mathbf{F} at a bifurcation point (y_0, μ_0) , (e.g. $\mathbf{F}_x^0, \mathbf{F}_\mu^0, \dots$), and these can be evaluated in terms of the derivatives of the original vector field as $\mathbf{F}_x^0 = \mathbf{G}_y^0$, $\mathbf{F}_\mu^0 = \mathbf{G}_y^0 (dy_E/d\mu)_0 + \mathbf{G}_\mu^0$, and so on.

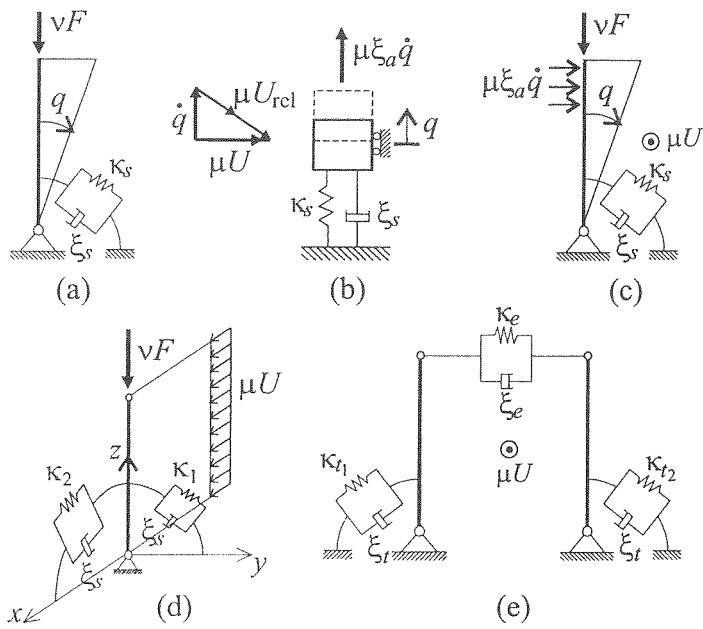


Figure 2. Sample structures exhibiting: (a) divergence, (b) Hopf bifurcation, (c) double-zero bifurcation, (d) Hopf-divergence, (e) double-Hopf.

3.2. Hopf bifurcation

The aerolastic oscillator in Fig. 2b is a prototype for the Hopf bifurcation. If the oscillator is subjected to a wind flow of uniform velocity μU , an aerodynamic force $\mu \xi_a \dot{q}$ acting transversally to the flow arises [29]. The variational equation based on the equilibrium position $q = 0$ still leads to Eq. (3) with $\kappa = \kappa_s$ being the elastic stiffness and $\xi = \xi_s - \mu \xi_a$ the total damping, where ξ_s and $\mu \xi_a$ are the structural damping and the aerodynamic damping respectively, the latter being positive for aerodynamically unstable cross-section shapes. For small wind velocities, the eigenvalues are stable, but when μ is equal to the critical value $\mu_c = \xi_s / \xi_a$, the total damping vanishes. The complex eigenvalues correspondingly cross the imaginary axis (Fig. 1b).

3.3. Double-zero bifurcation

A combination of the two previous mechanisms of bifurcation leads to the double-zero bifurcation. The same structure as Fig. 2a is considered, but is now additionally loaded with a wind flow μU orthogonal to the plane of the structure (Fig. 2c). The wind produces aerodynamic forces in this plane of the type $\mu \xi_a \dot{q}$, so that Eq. (3) still holds, but with $\xi = \xi_s - \mu \xi_a$ and $\kappa = \kappa_s - \nu \kappa_g$. By varying the two control parameters μ and ν , the whole (κ, ξ) -plane is spanned, so that it is more convenient to assume these latter as control parameters. By discussing the nature of the roots of the eigenvalue problem (3), the

scenario of Fig. 3 is found. The equilibrium position is stable in the quadrant $\xi > 0, \kappa > 0$ and unstable elsewhere. The ξ -axis is the locus of divergence \mathcal{D} , since one of the eigenvalues vanishes on it; moreover, the positive κ -half-axis is the locus of the Hopf bifurcation \mathcal{H} , since the eigenvalues are purely imaginary on it. In contrast, on the negative κ -half-axis the eigenvalues are both real, of the type $\lambda = \pm\alpha$. *The Hopf bifurcation boundary therefore dies at the crossing with the divergence boundary.* At the intersection $(\kappa, \xi) = (0, 0)$ the system has a double-zero eigenvalue, so that a double-zero codimension-2 bifurcation (Fig. 1c) takes place there.

At the bifurcation, the Jacobian matrix reduces to the 2×2 Jordan block:

$$J = \begin{pmatrix} 0 & 1 \\ 0 & 0 \end{pmatrix} \quad (4)$$

Since this matrix admits the unique eigenvector $(q, \dot{q}) = (1, 0)$, the system is *defective* or *nilpotent*. This circumstance is general, for nonconservative systems: eigenvalues of algebraic multiplicity greater than 1 have lower (generally 1) geometric multiplicity, and consequently an incomplete set of eigenvectors exists. This characteristic has some repercussion on the analytical treatment of such bifurcations, as will be explained below. Figure 3 shows that the defective double-zero point is not isolated, but belongs to a family $\mathcal{N} := \{(\kappa, \xi) \mid \kappa = \xi^2/4\}$ of nilpotent systems in which the eigenvalues are real and coincident, stable or unstable. Curve \mathcal{N} organizes the eigenvalues in both the stable and unstable zones, by separating over- and under-critically damped systems.

To sum up, the example shows that the double-zero bifurcation *does not* occur at the intersection of two divergence boundaries, as one might naively expect. Indeed, for a general N -dimensional system, this bifurcation occurs when the two invariants of the Jacobian matrix of higher order, I_N and I_{N-1} , simultaneously vanish. Now, while $I_N = 0$ is a locus of divergence, no eigenvalue properties are associated with $I_{N-1} = 0$. In contrast, the bifurcation is caused by a degeneracy of a Hopf bifurcation in which, along the Hopf-

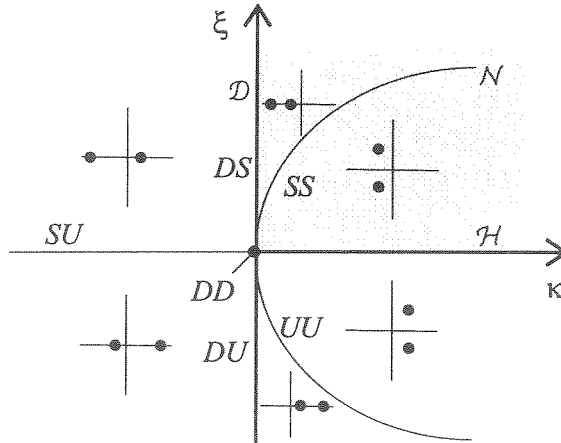


Figure 3. Linear stability diagram for the one-d.o.f. system in Fig. 2c; \mathcal{D} divergence boundary, \mathcal{H} Hopf boundary, \mathcal{N} nilpotent system locus; D, S, U : zero, stable, unstable real eigenvalues.

boundary, the two imaginary critical eigenvalues collapse in a double-zero eigenvalue. Thus, the death of the Hopf boundary and the branching off of the divergence boundary are explained. This kind of general mechanism of bifurcation is known as Takens-Bogdanova. Other mechanism leading to the double-zero eigenvalue (only one Hopf boundary, two divergence boundaries or all three boundaries) are also possible [30]; however they occur when *the derivatives* $\kappa_{,\mu}$ and $\kappa_{,\nu}$ *of the stiffness coefficient* κ *in Eq. (3) simultaneously vanish at the bifurcation point* and therefore refer to non-generic cases, of higher codimension.

Non-generic double-divergence bifurcations are often encountered in the theory of elastic buckling [31-34] and are known as *simultaneous buckling modes*. Such bifurcation occurs when two (or more) different forms of buckling (e.g. occurring in two different planes, or in a ‘local’ and a ‘global’ pattern [35]) manifest themselves at the same value of the load parameter ν . Typically, the tuning between the two critical loads is obtained by adjusting a geometrical parameter ρ , which therefore plays the role of second bifurcation parameter. A classical example is given by Augusti’s model [36] (see Fig. 2d, with $\mu = 0$), for which the eigenvalue problem reads:

$$\begin{bmatrix} \lambda^2 + \xi_x \lambda + \kappa_x & 0 \\ 0 & \lambda^2 + \xi_y \lambda + \kappa_y \end{bmatrix} \begin{pmatrix} \vartheta_x \\ \vartheta_y \end{pmatrix} = \begin{pmatrix} 0 \\ 0 \end{pmatrix} \quad (5)$$

where $\kappa_x = \kappa_1 - \nu \kappa_g$, $\kappa_y = \kappa_2 - \nu \kappa_g$, $\xi_x = \xi_y = \xi_s$, with $\rho := \kappa_2 / \kappa_1$ the tuning parameter. The invariants of higher order are: $I_4 = \kappa_x \kappa_y$ and $I_3 = \xi_x \kappa_y + \xi_y \kappa_x$. At the C-point $(\nu, \rho) = (\kappa_1 / \kappa_g, 1)$ of the parameter space it is $I_3 = I_4 = 0$ and a double-zero eigenvalue therefore exists. In addition $I_{4,\nu} = I_{4,\rho} = 0$ hold, i.e. the manifold $I_4 = 0$ bifurcates at C; however, this condition alone would not entail a double divergence at C if I_3 did not vanish at the same point.

3.4. Hopf-divergence bifurcation

The two-d.o.f. system in Fig. 2d is considered, consisting of a hinged rigid rod, elastically restrained and damped in two orthogonal planes, subjected to a dead load νF and a wind flow μU . The two loads are first considered separately. Due to the dead load, two modes of divergence can occur in any of the two planes; however, by assuming $\kappa_1 \gg \kappa_2$, the lower mode manifests itself in the (x, z) -plane at $\nu = \nu_c$. The wind flow, in contrast, causes a Hopf bifurcation and, consequently, triggers a motion in the (y, z) -plane at $\mu = \mu_c$. When the two loads act simultaneously, due to drag forces $\eta \mu^2$ produced by the wind in the (x, z) -plane, the trivial position $(\vartheta_x, \vartheta_y) = (0, 0)$ is no longer of equilibrium, and the system experiences a rotation $\vartheta_y = \vartheta_y(\mu)$ around the y -axis. Such an effect destroys the trivial fundamental path, and the drag coefficient η is therefore an *imperfection parameter*. If η is small, as is the case with aerodynamic cross-sections shapes of the rod, it is convenient to consider the real system as a perturbation of an ideal (although non-existent) perfect system having zero-drag coefficient η . Hence, the problem is analyzed in the (μ, ν, η) -space of two bifurcation and one imperfection parameters; it is also assumed that $\eta \ll (\mu, \nu)$. The bifurcation of the perfect system is

first studied and the effect of the imperfection is only introduced in the analysis of the post-critical behavior.

The stability of the trivial equilibrium position is governed by the eigenvalue problem (5) in which $\kappa_x = \kappa_1 - v \kappa_g$, $\kappa_y = \kappa_2 - v \kappa_g$, $\xi_x = \xi_s - \xi_d \mu$, $\xi_y = \xi_s + \xi_d \mu$, with $\xi_a > 0$, $\xi_d > 0$ aerodynamic coefficients. On the (μ, v) -plane (Fig. 4) the lines $v = v_c := \kappa_2 / \kappa_g$ and $\mu = \mu_c := \xi_s / \xi_a$ represent codimension-1 bifurcations, of divergence \mathcal{D} and Hopf \mathcal{H} , respectively. Their intersection point $C \equiv (\mu_c, v_c)$ is a codimension-2 critical point at which a Hopf-divergence takes place.

It is worth noticing that, as in the double-zero bifurcation, the critical point C is located at the intersection of a Hopf- and a divergence-boundary. However, in contrast to the former case, the *Hopf-boundary now crosses the divergence boundary*, and does not die at the intersection. Thus, while at the double-zero bifurcation a unique critical mode exists, at the Hopf-divergence, two distinct critical modes exist, a buckling mode in the (x, z) -plane, and a harmonic motion in the (y, z) -plane, which still survives if μ exceeds its critical value. Such a property is general, since at the Hopf-divergence bifurcation, the canonical form of the Jacobian contains a diagonal 3×3 block of the type $\text{diag}\{0, i\omega, -i\omega\}$. Since all the critical eigenvalues are simple, one real and a couple of complex conjugate eigenvectors are associated with them.

3.5. Double-Hopf bifurcation

A more complex 2-d.o.f. system is considered to illustrate the mechanism of the double-Hopf bifurcation. The system in Fig. 2e consists of two rigid rods, elastically restrained and damped against in-plane rotations, connected at the free ends by an elasto-viscous extensional device, able to furnish forces of both signs for a given strain (e.g. an active control device). The system is then subjected to a wind flow blowing orthogonally to the plane of the structure. Due to the mechanism of the aerodynamic forces, both rods, considered independently, experience Hopf bifurcations; due to the presence of the coupling device, they interact.

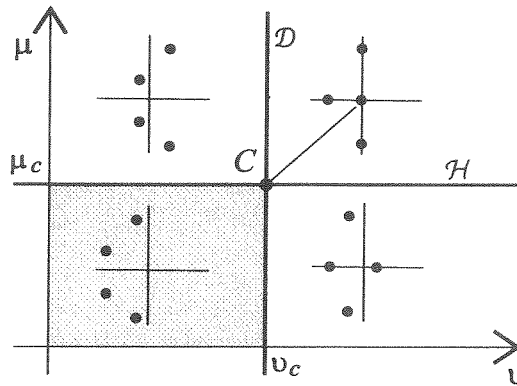


Figure 4. Linear stability diagram for the two-d.o.f. in Fig. 2d.

The eigenvalue problem governing the stability of the trivial equilibrium position reads:

$$\begin{bmatrix} \lambda^2 + \lambda \xi & -\lambda \xi_e - \kappa_e \\ + \kappa_{t1} + \kappa_e & \\ \hline -\lambda \xi_e - \kappa_e & \lambda^2 + \lambda \xi \\ & + \kappa_{t2} + \kappa_e \end{bmatrix} \begin{pmatrix} \vartheta_1 \\ \vartheta_2 \end{pmatrix} = \begin{pmatrix} 0 \\ 0 \end{pmatrix} \quad (6)$$

where $\xi := \xi_e + \xi_t - \mu \xi_a$ accounts for the effects of the extensional, torsional and aerodynamic damping and ϑ_1 and ϑ_2 are the (linearized) rotations of the two rods.

A first family of systems (6) displaying most of the peculiar aspects of the phenomenon is represented by *symmetric systems* ($\kappa_{t1} = \kappa_{t2} =: \kappa_t$). In this case Eqs. (6) admit the solutions $(\vartheta_1, \vartheta_2) = (1, 1)$ (antisymmetric mode, in which the rods are in-phase) and $(\vartheta_1, \vartheta_2) = (1, -1)$ (symmetric mode, in which the rods are in counter-phase). In the antisymmetric mode the extensional device is not stretched, so that the two rods behave as if they were independent; they undergo a Hopf bifurcation when their total damping vanishes, i.e. at $\mu = \mu_1 := \xi_t / \xi_a$. In contrast, in the symmetric mode, the extensional device increases (decreases) the total damping if $\xi_e > 0$ ($\xi_e < 0$) and the Hopf bifurcation manifests at $\mu = \mu_2 := (\xi_t + 2\xi_e) / \xi_a$. There thus exist two Hopf boundaries \mathcal{H}_i ($i = 1, 2$) on the (μ, ξ_e) -plane of the bifurcation parameters (Fig. 5), each associated with the frequencies $\omega_1 = \sqrt{\kappa_t}$ and $\omega_2 = \sqrt{\kappa_t + 2\kappa_e}$. They cross each other at $(\mu_c, \xi_{ec}) := (\xi_t / \xi_a, 0)$ where a double-Hopf bifurcation takes place. For generic values of the ratio $\rho := (\kappa_e / \kappa_t) > 0$ for which ω_2 / ω_1 is not an integer, the bifurcation is *nonresonant* (of codimension-2), while for special values of the ratio ρ , the bifurcation is *resonant* (of codimension-3) of 1:1, 1:2, 1:3, ..., type. In these cases ρ plays the role of third bifurcation parameter. Since it does not affect the type of the eigenvalues, the stability diagram in the three-dimensional space simply comprises two planes parallel to the ρ -axis, whose trace on the (ξ_e, μ) -plane is represented in Fig. 5.

One disadvantage of the example discussed is that the 1:1 resonant system belonging

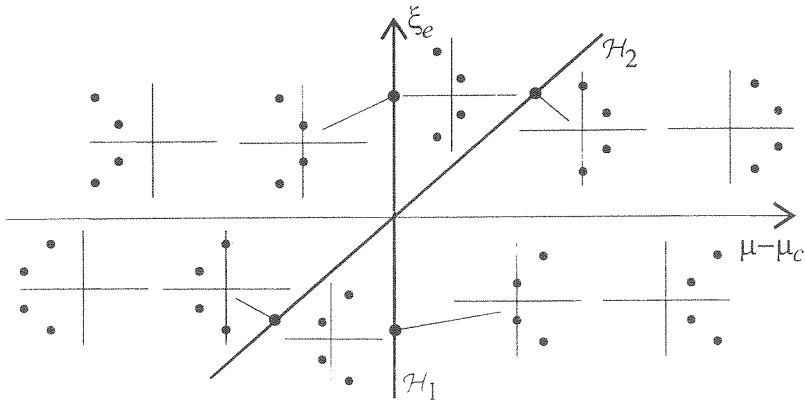


Figure 5. Linear stability diagram for the two-rod system in Fig. 2c.

to the family of symmetric structures does not represent a generic case. Indeed it occurs for $\mu = \mu_c$, $\kappa_e = 0$, $\xi_e = 0$, for which the two rods are uncoupled; this circumstance means that two independent modes $(\vartheta_1, \vartheta_2) = (1, 0)$ and $(0, 1)$ exist at the bifurcation (non-defective system). In the generic case, in contrast, a 1:1 resonant system undergoing double-Hopf bifurcation possesses only one critical complex eigenvector (defective system), since its Jacobian contains the Jordan block:

$$J = \begin{pmatrix} i\omega & 1 \\ 0 & i\omega \end{pmatrix} \quad (7)$$

and its conjugate. To obtain a system exhibiting such a generic bifurcation it is therefore necessary to resort to *non symmetric systems* ($\kappa_{l1} \neq \kappa_{l2}$). In order for Eqs. (6) to admit two imaginary solutions $\lambda = (\pm i\omega_1, \pm i\omega_2)$, the characteristic equation must be of the type $(\lambda^2 + \omega_1^2)(\lambda^2 + \omega_2^2) = 0$, i.e. odd powers of λ must vanish. This occurs when two conditions hold simultaneously: (a) $\xi = 0$, i.e. $\mu = \mu_c := (\xi_l + \xi_e)/\xi_a$ and, (b) $\kappa_e \xi_e = 0$. Two sub-families therefore follows from condition (b); by taking, for example, $\kappa_e = 0$, special values of the ratio $\rho := \kappa_{l1}/\kappa_{l2} > 0$ are found for which the critical frequencies are in ratios of 1:1, as well as 1:2, 1:3, ..., [25]. By fixing the auxiliary parameter $\kappa_{l2} = 1$, they are: $\rho_c := (1 \pm \xi_e)^2$, $4 + O(\xi_e^2)$, $9 + O(\xi_e^2)$, ..., respectively. In the 1:1 resonant case only one complex mode $(\pm i\sqrt{1 \pm \xi_e}, 1)$ is found, involving both rods in the motion. The resonant (nonsymmetric) systems belong to the space of the control parameters (μ, κ_e, ρ) and occur at the codimension-3 critical points $(\mu_c, 0, \rho_c)$.

The stability diagrams for (defective or not) resonant bifurcations cannot be derived in a simple way, but use must be made, for instance, of the Routh-Hurwitz criterion [37]. When these manifolds are represented in the (μ, κ_e, ρ) -parameter space, they appear as those in Fig. 6. The diagram in Fig. 6a shows two nearly-planar surfaces which are nearly independent of ρ . The diagram in Fig. 6b shows two surfaces intersecting each other at the positive $(\rho - \rho_c)$ -axis, along which nonresonant double-Hopf bifurcations occur; for $\rho = \rho_c$ the bifurcation is resonant.

4. Eigensolution sensitivities

Sensitivity analysis makes it possible to explore the behavior of the critical eigenvalues around the criticality when the bifurcation parameters are varied. It is useful in bifurcation analysis for the following reasons. (a) If only the bifurcation point is known but the critical boundaries containing it are unknown, sensitivity analysis enables us to build up asymptotic approximations of the boundaries. (b) If, on the other hand, the bifurcation point is unknown, but an approximation of it is known, sensitivity analysis guides the search for the exact point. (c) If a nonlinear analysis has been performed (see Sects. 5 to 7 below) and a new equilibrium point has been found in the neighborhood of the bifurcation point, sensitivity analysis make it possible to decide about the stability of the new point. In addition to these computational motivations, there is another good reason

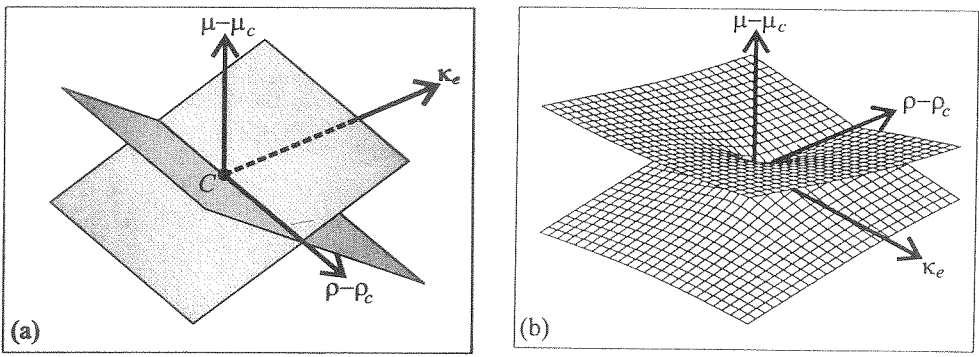


Figure 6. Critical manifolds for: (a) non-defective (1:2, 1:3, ...) resonant double-Hopf; (b) defective (1:1) resonant double-Hopf.

for analyzing the sensitivity of the eigensolutions of a linear operator: the analysis has close similarities with the search for bifurcated solutions by a perturbation method and suggests the best strategy to tackle the problem in singular cases.

Let (y_0, μ_0) be a bifurcation point for the system (1) (at which the Jacobian $\mathbf{G}_y^0 := \mathbf{G}_y(y_0, \mu_0)$ admits one or more eigenvalues with zero real part) and let $y_E = y_E(\mu)$ be an equilibrium path (not necessarily the fundamental one) passing through the bifurcation point. Let us determine an asymptotic expression for the eigensolutions ($\lambda = \lambda(\mu)$, $w = w(\mu)$) along the path, i.e. let us solve the following eigenvalue problem:

$$[\mathbf{G}_y(y_E(\mu), \mu) - \lambda(\mu)]w(\mu) = 0 \quad (8)$$

asymptotically for $\mu \rightarrow \mu_0$. Let us decide to vary the control parameters μ proportionally to a perturbation parameter ε , namely $\mu = \mu_0 + \varepsilon \hat{\mu}$, with $\hat{\mu} = O(1)$, so that $\lambda = \lambda(\varepsilon)$, $w = w(\varepsilon)$. From a geometric point of view the choice corresponds to spanning the neighborhood of the bifurcation point by straight lines. Two cases are analyzed, according to the multiplicity of the eigenvalues at (y_0, μ_0) , namely non-defective and defective eigenvalues.

4.1. Non-defective eigenvalue

Let us first assume that \mathbf{G}_y^0 admits a critical eigenvalue λ_{0j} having algebraic multiplicity $m = 1$. By expanding the eigensolution $(\lambda(\varepsilon), w(\varepsilon))$ in Mac Laurin series:

$$\begin{aligned} w &= w_0 + \varepsilon w_1 + \frac{\varepsilon^2}{2} w_2 + \dots \\ \lambda &= \lambda_0 + \varepsilon \lambda_1 + \frac{\varepsilon^2}{2} \lambda_2 + \dots \end{aligned} \quad (9)$$

differentiating Eq. (8) with respect to ε , and evaluating the derivatives at $\varepsilon=0$, the

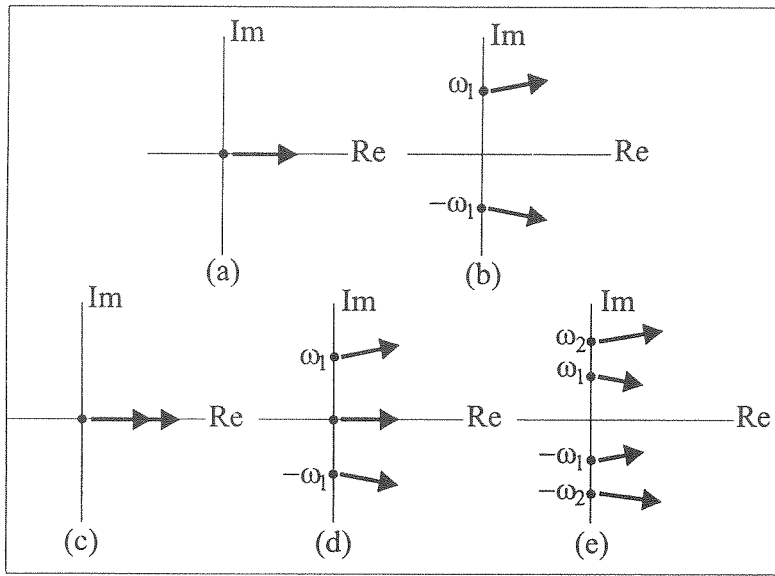


Figure 1. Simple and multiple bifurcations: (a) divergence, (b) Hopf, (c) double-zero, (d) Hopf-divergence, (e) double-Hopf.

This property is demonstrated by the method illustrated ahead.

3. Sample mechanical systems

Sample (perfect) systems exhibiting the bifurcations discussed above are presented and some mechanical aspects are discussed. Analysis is limited to linear stability, the nonlinear behavior being analyzed below.

3.1. Divergence

A 1-d.o.f. rigid bar, elastically restrained and damped, axially loaded with a compressive force (Fig. 2a) is the simplest model for divergence bifurcation (buckling). The equation of motion linearized around the trivial equilibrium solution $q = 0$ leads to the following eigenvalue problem:

$$(\lambda^2 + \xi\lambda + \kappa)q = 0 \tag{3}$$

where $\xi = \xi_s > 0$ is the structural damping and $\kappa = \kappa_s - \nu\kappa_g$ the total stiffness, where κ_s and $\nu\kappa_g$ are the (positive) elastic and geometric stiffnesses, respectively, and ν is the load multiplier. For small ν the eigenvalues are complex conjugate with negative real part, so that the equilibrium position is stable. When ν reaches the critical values $\nu_c = \kappa_s / \kappa_g$, the total stiffness vanishes and one eigenvalue crosses the zero, while the second remains stable. Thus the mechanism of Fig. 1a occurs.

following perturbation equations are obtained:

$$\begin{aligned}
(\mathbf{A}_0 - \lambda_0 \mathbf{I}) \mathbf{w}_0 &= \mathbf{0} \\
(\mathbf{A}_0 - \lambda_0 \mathbf{I}) \mathbf{w}_1 &= \lambda_1 \mathbf{w}_0 - \mathbf{A}_1 \mathbf{w}_0 \\
(\mathbf{A}_0 - \lambda_0 \mathbf{I}) \mathbf{w}_2 &= \lambda_2 \mathbf{w}_0 + 2\lambda_1 \mathbf{w}_1 - \mathbf{A}_2 \mathbf{w}_0 - 2\mathbf{A}_1 \mathbf{w}_1
\end{aligned} \tag{10}$$

where

$$\begin{aligned}
\mathbf{A}_0 &:= \mathbf{G}_y^0, \quad \mathbf{A}_1 := \left(\mathbf{G}_{yy}^0 \left(\frac{dy_E}{d\mu} \right)_0 + \mathbf{G}_{y\mu}^0 \right) \hat{\boldsymbol{\mu}} \\
\mathbf{A}_2 &:= \left(\mathbf{G}_{yyy}^0 \left(\frac{dy_E}{d\mu} \right)_0^2 + 2\mathbf{G}_{yy\mu}^0 \left(\frac{d^2 y_E}{d\mu^2} \right)_0 + \mathbf{G}_{y\mu\mu}^0 \right) \hat{\boldsymbol{\mu}}^2
\end{aligned} \tag{11}$$

Equation (10₁) admits the solution $(\lambda_0, \mathbf{w}_0) = (\lambda_{0j}, \mathbf{u}_j)$, with $\lambda_{0j} = 0$ or $\lambda_{0j} = i\omega_j$ and \mathbf{u}_j the associate critical eigenvector. Eq. (10₂) then reads:

$$(\mathbf{A}_0 - \lambda_{0j} \mathbf{I}) \mathbf{w}_1 = \lambda_1 \mathbf{u}_j - \mathbf{A}_1 \mathbf{u}_j \tag{12}$$

Since the operator is singular, Eq. (12) admits a solution if and only if the known term is orthogonal to the solution of the homogeneous adjoint problem $(\mathbf{A}_0 - \lambda_{0j} \mathbf{I})^H \mathbf{v}_j = \mathbf{0}$ (H denoting the transpose conjugate), i.e. to the left eigenvector \mathbf{v}_j . From this solvability condition λ_1 is drawn:

$$\lambda_1 = \mathbf{v}_j^H \mathbf{A}_1 \mathbf{u}_j \tag{13}$$

having adopted the normalization $\mathbf{v}_j^H \mathbf{u}_j = 1$; λ_1 is called the first-order sensitivity of the j -th eigenvalue. Equation (12) can be solved (to within an arbitrary quantity) and the solution substituted in Eq. (10₃). By again enforcing solvability, λ_2 is obtained, and the procedure can be continued to any order.

4.2. Defective eigenvalue

Let us assume now that λ_{0j} has algebraic multiplicity $m > 1$, its geometric multiplicity being still equal to 1 (generic case). Since only one eigenvector \mathbf{u}_j is associated with λ_{0j} , the eigenvalue (and therefore the matrix \mathbf{A}_0) is *defective* (or nilpotent). It is known from algebra (see e.g. [38]) that a chain of m generalized (right) eigenvectors can be built-up to complete the base, by recursively solving the following equations:

$$(\mathbf{A}_0 - \lambda_{0j} \mathbf{I}) \mathbf{u}_{jk} = \mathbf{u}_{j,k-1} \quad k = 2, 3, \dots, m \tag{14}$$

with $\mathbf{u}_{j,1} \equiv \mathbf{u}_j$ the proper eigenvector. Equation (14) means that *all the eigenvectors of the*

chain, except for the higher-order eigenvector \mathbf{u}_{jm} , belongs to the range of the operator $\mathbf{A}_0 - \lambda_{0j}\mathbf{I}$, while \mathbf{u}_{jm} is external to it. By denoting by \mathbf{v}_{jm} the unique proper left eigenvector (i.e. the kernel of the homogeneous adjoint problem) $\mathbf{v}_{jm}^H \mathbf{u}_{jk} = \delta_{km}$ is obtained.

It is easy to see that the above procedure, which was successful when $m = 1$, fails when $m > 1$. Indeed, the solvability condition of Eq.(10₂) requires $\mathbf{v}_{jm}^H (\lambda_1 \mathbf{u}_{j1} - \mathbf{A}_1 \mathbf{u}_{j1}) = 0$. Since $\mathbf{v}_{jm}^H \mathbf{u}_{j1} = 0$, such a condition cannot be satisfied in the generic case $\mathbf{v}_{jm}^H \mathbf{A}_1 \mathbf{u}_{j1} \neq 0$. The reason for the drawback lies in the fact that integer power expansions of the eigensolutions were used, while defective matrices call for *fractional power expansions* [39]. As an example, if the (2, 1)-element of the block in Eq. (4) is perturbed by ε , the double-zero eigenvalue changes to $\lambda = \pm\varepsilon^{1/2}$. Defective matrices are therefore *highly sensitive to perturbations*, since the variations in their eigenvalues are larger than the perturbations.

The problem at hand is solved by replacing series (9) by (see [40] for more general cases):

$$\begin{aligned} \mathbf{w} &= \mathbf{w}_0 + \varepsilon^{1/m} \mathbf{w}_1 + \varepsilon^{2/m} \mathbf{w}_2 + \dots \\ \lambda &= \lambda_0 + \varepsilon^{1/m} \lambda_1 + \varepsilon^{2/m} \lambda_2 + \dots \end{aligned} \quad (15)$$

which leads to the following perturbation equations:

$$\begin{aligned} \varepsilon^0 : (\mathbf{A}_0 - \lambda_0 \mathbf{I}) \mathbf{w}_0 &= \mathbf{0} \\ \varepsilon^{1/m} : (\mathbf{A}_0 - \lambda_0 \mathbf{I}) \mathbf{w}_1 &= \lambda_1 \mathbf{w}_0 \\ \varepsilon^{2/m} : (\mathbf{A}_0 - \lambda_0 \mathbf{I}) \mathbf{w}_2 &= \lambda_1 \mathbf{w}_1 + \lambda_2 \mathbf{w}_0 \\ &\dots\dots\dots \\ \varepsilon : (\mathbf{A}_0 - \lambda_0 \mathbf{I}) \mathbf{w}_m &= \lambda_1 \mathbf{w}_{m-1} + \lambda_2 \mathbf{w}_{m-2} + \mathbf{K} - \mathbf{A}_1 \mathbf{w}_0 \\ \varepsilon^{1+1/m} : (\mathbf{A}_0 - \lambda_0 \mathbf{I}) \mathbf{w}_{m+1} &= \lambda_1 \mathbf{w}_m + \lambda_2 \mathbf{w}_{m-1} + \mathbf{K} \end{aligned} \quad (16)$$

Equation (16₂) can now be solved for any λ_1 , since its known term \mathbf{u}_{j1} belongs to the range of the operator. By solving it, $\mathbf{w}_1 = \lambda_1 \mathbf{u}_{j2}$ is found, with λ_1 still undetermined. Similarly, the $\varepsilon^{2/m}$ -order equation can be solved for any λ_1 and λ_2 , since the known terms \mathbf{u}_{j2} and \mathbf{u}_{j1} are again in the range of the operator. By solving Eq.(16₃) $\mathbf{w}_2 = \lambda_1^2 \mathbf{u}_{j3} + \lambda_2 \mathbf{u}_{j2}$ follows. By proceeding to higher orders, a solvability condition is first required at the ε -order, where *the highest element of the chain \mathbf{u}_{jm} appears together with the perturbation $\mathbf{A}_1 \mathbf{u}_{j1}$* . By requiring orthogonality to \mathbf{v}_{jm} , the following *nonlinear equation* is drawn:

$$\lambda_1^m = \mathbf{v}_{jm}^H \mathbf{A}_1 \mathbf{u}_{j1} \quad (17)$$

from which m roots are found (first-order sensitivities of the m coincident eigenvalues λ_{0j}). At higher-orders, in contrast, *linear equations* of the type $\lambda_2 \lambda_1^{m-1} = f(\lambda_1)$, $\lambda_3 \lambda_1^{m-1} = f(\lambda_1, \lambda_2), \dots$ are found, from which *one* value of $\lambda_2, \lambda_3, \dots$ is drawn for *each* of the m first-order sensitivities.

The procedure illustrated breaks down if $\lambda_1 = 0$ (or if it is small), since the subsequent solvability conditions vanish identically. This circumstance always manifests itself when the complete ball around the bifurcation point is explored in the parameter space, since, by recalling Eqs. (17) and (11₂), λ_1^m is the equation of a hyperplane in the parameter space (see [30] for further details). Therefore, it seems more convenient, to combine all the solvability conditions in a unique algebraic equation of degree m , valid in the whole ball:

$$\Delta\lambda_j^m + c_1(\boldsymbol{\mu})\Delta\lambda_j^{m-1} + \dots + c_m(\boldsymbol{\mu}) = 0 \quad (18)$$

where $\Delta\lambda_j := \lambda_j - \lambda_{j0}$. Thus, if $c_m = O(\varepsilon)$, then $\Delta\lambda_j = O(\varepsilon^{1/m})$; if $c_m < O(\varepsilon)$ then $\Delta\lambda_j > O(\varepsilon^{1/m})$. Equation (18) will be referred to as the *reconstituted sensitivity equation*, in analogy with the reconstituted bifurcation equation to be discussed later.

In conclusion, the sensitivities of a defective eigenvalue of algebraic multiplicity m are governed by an algebraic equation of degree m . *The solution furnished by the perturbation method is the series solution of this equation.*

The previous property mainly is based on the fact that the passive noncritical eigenvalues are supposed to be well-separated from the critical eigenvalues. As an example, the perturbed eigenvalue problem for a three-dimensional system (in Jordan canonical form) admitting the double root $\lambda_0 = 0$ calls for the solution of the following characteristic equation:

$$\left\| \begin{array}{cc|c} \varepsilon_{11} - \lambda & 1 + \varepsilon_{12} & \varepsilon_{13} \\ \varepsilon_{21} & \varepsilon_{22} - \lambda & \varepsilon_{23} \\ \hline \varepsilon_{31} & \varepsilon_{32} & \lambda_3 - \lambda + \varepsilon_{33} \end{array} \right\| = 0 \quad (19)$$

where $\lambda_3 = O(1)$ is the stable eigenvalue, and $\varepsilon_{ij} = O(\varepsilon)$ are perturbations (see [40] for a more general example). If the effects of the stable eigenvalue are ignored and only the perturbed Jordan block is considered, the algebraic equation of degree 2, $\Delta_2(\lambda) = 0$, is drawn, admitting the roots: $\lambda_{1,2}^* = O(\varepsilon^{1/2})$. If the whole matrix is considered, the cubic equation

$$(\lambda_3 - \lambda + \varepsilon_{33}) \Delta_2(\lambda) + \varepsilon_{31} \varepsilon_{23} + O(\varepsilon^2 \lambda, \varepsilon^3) = 0 \quad (20)$$

instead has to be satisfied. However, since $\lambda \ll \lambda_3$, it admits roots which are perturbation of $\lambda = \lambda_{1,2}^*$ and $\lambda = \lambda_3$. Since *we are interested only in the two roots of order $\varepsilon^{1/2}$* , Eq. (20) can be approximated by:

$$\Delta_2(\lambda) + \frac{\varepsilon_{31} \varepsilon_{23}}{\lambda_3} + O(\varepsilon^2 \lambda, \varepsilon^3) = 0 \quad (21)$$

which is still a 2-degree equation. Therefore, higher orders approximations only modify the coefficients of the lower-order equation. In a more general case in which more passive critical eigenvalues exist, terms of order $O(\varepsilon^2 \lambda^k)$ with $k = 2, 3, \dots$ are added to Eq. (21). However, although Eq. (21) becomes of higher degree, the coefficients of the powers of λ

greater than 2 are small. Therefore it is convenient to consider these high-order terms as perturbations of the degree-2 equation and solving the problem by a recursive method. In [41] an alternative method based on a Center-Manifold-like procedure is applied, showing the validity of the reduction to a low-order equation in the most general case of a defective matrix.

5. Multiple scale method for non-defective bifurcations

It is known [1-4] that the essential aspects of the behavior of multidimensional systems around bifurcation points are captured by a small set of bifurcation equations, equal in number to the (linear) codimension of the problem. The most common method to obtain such a reduced equation consists in applying the Center Manifold Method in connection with Normal Form Theory [2,3]; here an alternative approach, based on the Multiple Scale Method (MSM) [10] is instead illustrated. Perfect bifurcations are first analyzed and the effects of imperfections are then briefly described.

5.1. Jacobian spectral properties

Equations of motion reduced to the local form are considered, namely:

$$\dot{\mathbf{x}} = \mathbf{F}(\mathbf{x}, \boldsymbol{\mu}) \quad \mathbf{x} \in \mathbb{R}^N, \boldsymbol{\mu} \in \mathbb{R}^M \quad (22)$$

admitting the trivial solution $\mathbf{x} = \mathbf{0}, \forall \boldsymbol{\mu}$. Let us assume that $(\mathbf{x}, \boldsymbol{\mu}) = (\mathbf{0}, \mathbf{0})$ is a codimension- M bifurcation point O , at which the Jacobian $\mathbf{F}_x^0 := \mathbf{F}_x(\mathbf{0}, \mathbf{0})$ admits several critical eigenvalues, the remaining being stable. Let N_r be the number of real eigenvalues $\lambda_{0k} = 0$ ($k = 1, \dots, N_r$) and $2N_c$ the number of complex conjugate eigenvalues $\lambda_j = \pm i\omega_j$, ($j = 1, \dots, N_c$) so that $N_r + N_c + R = M$, with R being the number of resonance conditions. Such a bifurcation is defective if some eigenvalues have algebraic multiplicity greater than 1, i.e. if $N_r > 1$ and/or some imaginary eigenvalues are in 1:1 resonance conditions. Since defective bifurcations require special treatment, similarly to sensitivity analysis, non-defective bifurcations are first analyzed.

It is assumed that no more than one zero-eigenvalue exists at the bifurcation (i.e. $N_r = 0, 1$); moreover, coalescences among the imaginary eigenvalues $\lambda_j = \pm i\omega_j$ are excluded. Complete sets of right and left eigenvectors therefore exist, satisfying the following linear algebraic equations respectively,

$$\mathbf{F}_x^0 \mathbf{u}_0 = \mathbf{0}, \quad \mathbf{F}_x^0 \mathbf{u}_j = i\omega_j \mathbf{u}_j \quad (23)$$

and

$$(\mathbf{F}_x^0)^T \mathbf{v}_0 = \mathbf{0}, \quad (\mathbf{F}_x^0)^H \mathbf{v}_j = -i\omega_j \mathbf{v}_j \quad (24)$$

together with the complex conjugate eigenvectors $\mathbf{u}_{N_c+j} = \bar{\mathbf{u}}_j$, $\mathbf{v}_{N_c+j} = \bar{\mathbf{v}}_j$ ($j = 1, 2, \dots, N_c$). Right and left eigenvectors are orthonormalized according to $\mathbf{v}_h^H \mathbf{u}_k = \delta_{hk}$. In contrast, no restrictions are introduced about possible resonance conditions among the critical frequencies, given that they do not affect the completeness of the system eigenvectors at the criticality. General conditions of the type:

$$\sum_{j=1}^{N_c} k_{ij} \omega_j = 0 \quad i = 1, 2, \dots, R \quad (25)$$

are considered, where k_{ij} are small integer resonance coefficients.

5.2. Perturbation equations

A monoparametric family of solutions to Eq. (22), namely $\{\mathbf{x} = \mathbf{x}(t, \boldsymbol{\mu}(\varepsilon)), \boldsymbol{\mu} = \boldsymbol{\mu}(\varepsilon)\}$, is sought in the form of Mac Laurin series [14]:

$$\begin{pmatrix} \mathbf{x}(t) \\ \boldsymbol{\mu} \end{pmatrix} = \sum_{k=1}^{\infty} \frac{\varepsilon^k}{k!} \begin{pmatrix} \mathbf{x}_k(t) \\ \boldsymbol{\mu}_k \end{pmatrix} \quad (26)$$

with ε being a perturbation parameter. Moreover, according to the MSM, the state variables \mathbf{x} (and therefore their derivatives \mathbf{x}_k at $\varepsilon=0$) are assumed to depend on several independent temporal scales:

$$t_0 = t, \quad t_1 = \varepsilon t, \quad t_2 = \frac{\varepsilon^2}{2!} t, \dots, \quad t_k = \frac{\varepsilon^k}{k!} t \quad (27)$$

so that the time-derivative is expressed by the chain rule:

$$\frac{d}{dt} = d_0 + \varepsilon d_1 + \frac{\varepsilon^2}{2!} d_2 + \dots + \frac{\varepsilon^k}{k!} d_k \quad (28)$$

with $d_k := \partial/\partial t_k$. By differentiating Eq. (22) $k=1, 2, \dots$ times with respect to the perturbation parameter ε , evaluating the derivatives at $\varepsilon=0$ and using Eqs. (26) and (28), the perturbation equations follow. Up to the ε^3 - order they read:

$$\begin{aligned} (d_0 - \mathbf{F}_x^0) \mathbf{x}_1 &= \mathbf{0} \\ (d_0 - \mathbf{F}_x^0) \mathbf{x}_2 &= \mathbf{F}_{xx}^0 \mathbf{x}_1^2 + 2\mathbf{F}_{x\boldsymbol{\mu}}^0 \mathbf{x}_1 \boldsymbol{\mu}_1 - 2d_1 \mathbf{x}_1 \\ (d_0 - \mathbf{F}_x^0) \mathbf{x}_3 &= 3\mathbf{F}_{xx}^0 \mathbf{x}_1 \mathbf{x}_2 + 3\mathbf{F}_{x\boldsymbol{\mu}}^0 \mathbf{x}_2 \boldsymbol{\mu}_1 + 3\mathbf{F}_{x\boldsymbol{\mu}}^0 \mathbf{x}_1 \boldsymbol{\mu}_2 + 3\mathbf{F}_{xx\boldsymbol{\mu}}^0 \mathbf{x}_1^2 \boldsymbol{\mu}_1 \\ &\quad + 3\mathbf{F}_{x\boldsymbol{\mu}\boldsymbol{\mu}}^0 \mathbf{x}_1 \boldsymbol{\mu}_1^2 + \mathbf{F}_{xxx}^0 \mathbf{x}_1^3 - 3d_2 \mathbf{x}_1 - 3d_1 \mathbf{x}_2 \end{aligned} \quad (29)$$

In Eqs. (29) $\mathbf{F}_{xx}^0, \mathbf{F}_{x\boldsymbol{\mu}}^0, \dots$ are second- and higher-derivatives of vector \mathbf{F} with respect to vectors \mathbf{x} and $\boldsymbol{\mu}$, evaluated at the bifurcation point $O^{(8)}$. In deriving Eqs. (29) it has been taken into account that, since $\mathbf{F}(\mathbf{0}, \boldsymbol{\mu}) = \mathbf{0} \quad \forall \boldsymbol{\mu}$, all the $\boldsymbol{\mu}$ -derivatives of \mathbf{F} vanish, i.e. $\mathbf{F}_{\boldsymbol{\mu}}(\mathbf{0}, \boldsymbol{\mu}) = \mathbf{F}_{\boldsymbol{\mu}\boldsymbol{\mu}}(\mathbf{0}, \boldsymbol{\mu}) = \dots = \mathbf{0}$ and in particular, $\mathbf{F}_{\boldsymbol{\mu}}^0 = \mathbf{F}_{\boldsymbol{\mu}\boldsymbol{\mu}}^0 = \dots = \mathbf{0}$.

5.3. Solution to perturbation equations

Equation (29) are partial time-derivatives equations in the unknowns \mathbf{x}_k and $\boldsymbol{\mu}_k$. The non-decaying solution to equations (29₁) is a linear combination of the critical

⁽⁸⁾ From a computational point of view there is no need to build-up such large multi-dimensional matrices which usually contains many zeros. Rather, it is convenient to perform first the scalar product $\delta \mathbf{x}^T \mathbf{F}$ (virtual work) with $\delta \mathbf{x} = \{\delta x_1, \delta x_2, \dots, \delta x_n\}$ being a dummy vector, and then to perform the successive variations $\delta \mathbf{x}^T \mathbf{F}_{xx}^0 \mathbf{x}_1$, $\delta \mathbf{x}^T \mathbf{F}_{xx}^0 \mathbf{x}_1 \mathbf{x}_2$, $\delta \mathbf{x}^T \mathbf{F}_{x\boldsymbol{\mu}}^0 \mathbf{x}_1 \boldsymbol{\mu}_1$, and so on.

eigenvectors, whose arbitrary amplitudes depend on slow time scales:

$$\mathbf{x}_1 = \frac{1}{2} a_0(t_1, t_2, \kappa) \mathbf{u}_0 + \sum_{j=1}^{N_c} A_j(t_1, t_2, \kappa) \mathbf{u}_j e^{i\omega_j t_0} + c.c. \quad (30)$$

In Eq. (30) a_0 is a real quantity, while A_j are complex quantities, *c.c.* denoting complex conjugates.

By substituting \mathbf{x}_1 in the ‘known term’ of Eqs. (29₂), harmonic forcing terms of frequencies 0, ω_j and $\omega_i \pm \omega_k$ are found. The zero- and ω_j -harmonics represent resonant terms for the system; the combination $(\omega_i \pm \omega_k)$ -harmonics are instead generally nonresonant, *unless* $\omega_i \pm \omega_k = \omega_j$, according to the (second-order) resonance conditions (25). Therefore, Eq. (29₂) have the following form:

$$(d_0 - \mathbf{F}_x^0) \mathbf{x}_2 = (\mathbf{b}_{10} - \mathbf{u}_0 d_1 a_0) + 2 \sum_{j=1}^{N_c} (\mathbf{b}_{1j} - \mathbf{u}_j d_1 A_j) e^{i\omega_j t_0} + c.c. + NRT \quad (31)$$

where *NRT* stands for nonresonant terms and $\mathbf{b}_{10}, \mathbf{b}_{1j}$ are vectors including quadratic combinations of the first-order quantities $(a_0, A_j, \boldsymbol{\mu}_1)$. In order that Eq. (31) admit a non-diverging solution, the following (solvability) conditions must hold:

$$d_1 a_0 = \mathbf{v}_0^T \mathbf{b}_{10}, \quad d_1 A_j = \mathbf{v}_j^H \mathbf{b}_{1j}, \quad j = 1, 2, \kappa, N_c \quad (32)$$

requiring that the resonant forcing terms be orthogonal to the left eigenvectors of associated frequencies. By solving Eq. (29₂), \mathbf{x}_2 is found to be a linear combination of harmonics of frequencies 0, ω_j and $\omega_i \pm \omega_k$, where the arbitrary quantities included in the resonant terms can be put equal to zero or determined by normalization conditions.

By substituting \mathbf{x}_2 in the known terms of Eq. (29₃) and accounting for Eqs. (32) to express $d_1 \mathbf{x}_2$, the perturbation equation reads:

$$(d_0 - \mathbf{F}_x^0) \mathbf{x}_3 = 3/2 (\mathbf{b}_{20} - \mathbf{u}_0 d_2 a_0) + 3 \sum_{j=1}^{N_c} (\mathbf{b}_{2j} - \mathbf{u}_j d_2 A_j) e^{i\omega_j t_0} + c.c. + NRT \quad (33)$$

with $\mathbf{b}_{20}, \mathbf{b}_{2j}$ being cubic combinations of the first-order quantities $(a_0, A_j, \boldsymbol{\mu}_1)$ and the second-order quantity $\boldsymbol{\mu}_2$. In Eq. (33) second-order resonances (25) $\omega_i \pm \omega_h \pm \omega_k = 0$ or third-order resonances $\omega_i \pm \omega_h \pm \omega_k = \omega_j$ are considered. The solvability of Eq. (33) calls for the following conditions to be satisfied:

$$d_2 a_0 = \mathbf{v}_0^T \mathbf{b}_{20}, \quad d_2 A_j = \mathbf{v}_j^H \mathbf{b}_{2j}, \quad j = 1, 2, \dots, N_c \quad (34)$$

The procedure can be continued to higher-orders in the same way.

5.4. Amplitude modulation equations

Equations (32) and (34) govern, for given $\boldsymbol{\mu}_1$ and $\boldsymbol{\mu}_2$, the evolution of the amplitudes (a_0, A_j) on the slow scales t_1 and t_2 , and are therefore named Amplitude Modulation Equations (AME). An in-depth analysis of these equations reveals that they have the

following structure [42]:

$$\begin{aligned}
 d_1 a_0 &= \mathcal{L}_{10}(\boldsymbol{\mu}_1 a_0, a_0^2; A_l \bar{A}_l) \\
 d_1 A_j &= \mathcal{L}_{1j}(\boldsymbol{\mu}_1 A_j, a_0 A_j; A_i A_k, A_i \bar{A}_k) \\
 &\quad \forall l, \forall (i, k) | \omega_i \pm \omega_k = \omega_j
 \end{aligned} \tag{35}$$

and

$$\begin{aligned}
 d_2 a_0 &= \mathcal{L}_{20}(\boldsymbol{\mu}_2 a_0, \boldsymbol{\mu}_1^2 a_0, \boldsymbol{\mu}_1 a_0^2, a_0^3; \boldsymbol{\mu}_1 A_l \bar{A}_l, a_0 \bar{A}_l \bar{A}_l; A_i A_h A_k, A_i \bar{A}_h A_k, \mathcal{K}) \\
 d_2 A_j &= \mathcal{L}_{2j}(\boldsymbol{\mu}_2 A_j, \boldsymbol{\mu}_1^2 A_j, \boldsymbol{\mu}_1 a_0 A_j, a_0^2 A_j; A_j A_l \bar{A}_l; A_i A_h A_k, A_i \bar{A}_h A_k, \mathcal{K}) \\
 &\quad \forall l, \forall (i, h, k) | \omega_i \pm \omega_h \pm \omega_k = (0, \omega_j)
 \end{aligned} \tag{36}$$

where \mathcal{L}_{hk} are linear algebraic operators with complex constant coefficient. The arguments of \mathcal{L}_{hk} are homogeneous quadratic (if $h = 1$) or cubic (if $h = 2$) forms of $(a_0, A_j, \boldsymbol{\mu}_1; \boldsymbol{\mu}_2)$, the *frequencies associated with each term being equal to 0* (if $k = 0$) or ω_j (if $k = j$), i.e. they are resonant terms. Several terms in Eqs. (35) and (36) are independent of the resonance conditions (25), (e.g. $A_l \bar{A}_l$ in Eq. (35₁) has zero-frequency and $a_0^2 A_j$ in Eq. (36₂) has frequency ω_j) so that they are always included in the equations, even if the system is nonresonant; they have therefore been named *improper resonant terms* [42]. In contrast, several terms directly depend on the resonance conditions (25) (e.g. $A_i \bar{A}_k$ in Eq. (35₂) has frequency $\omega_i - \omega_k$) and appear in the AME only if specific relations among the critical frequencies occur; these have therefore been named *proper resonant terms* [42].

To put the complex equations in real form, the polar representation $A_j = 1/2 a_j \exp(i\vartheta_j)$ is adopted⁽⁸⁾, which transforms Eqs. (35) and (36) in two sets of $2N_c + 1$ unknowns (a_0, a_j, θ_j) , having the following form:

$$\begin{aligned}
 d_1 a_0 &= \mathcal{L}_{10}(\boldsymbol{\mu}_1 a_0, a_0^2; a_0^2) \\
 d_1 a_j &= \mathcal{R}_{1j}(\boldsymbol{\mu}_1 a_j, a_0 a_j; a_i a_k \exp(i\gamma_{ikj}), a_i a_k \exp(i\gamma_{i,-k,j}), \mathcal{K}) \\
 a_j d_1 \vartheta_j &= \mathcal{J}_{1j}(\boldsymbol{\mu}_1 a_j, a_0 a_j; a_i a_k \exp(i\gamma_{ikj}), a_i a_k \exp(i\gamma_{i,-k,j}), \mathcal{K})
 \end{aligned} \tag{37}$$

and

$$\begin{aligned}
 d_2 a_0 &= \mathcal{L}_{20}(\boldsymbol{\mu}_2 a_0, \boldsymbol{\mu}_1^2 a_0, \boldsymbol{\mu}_1 a_0^2, a_0^3; \boldsymbol{\mu}_1 a_0^2, a_0 a_0^2; a_i a_h a_k \exp(i\gamma_{ihk}), \\
 &\quad a_i a_h a_k \exp(i\gamma_{i,-h,k}), \mathcal{K}) \\
 d_2 a_j &= \mathcal{R}_{2j}(\boldsymbol{\mu}_2 a_j, \boldsymbol{\mu}_1^2 a_j, \boldsymbol{\mu}_1 a_0 a_j, a_0^2 a_j; a_j a_0^2; a_i a_h a_k \exp(i\gamma_{ihkj}), \\
 &\quad a_i a_h a_k \exp(i\gamma_{i,-h,k,j}), \mathcal{K}) \\
 a_j d_2 \vartheta_j &= \mathcal{J}_{2j}(\boldsymbol{\mu}_2 a_j, \boldsymbol{\mu}_1^2 a_j, \boldsymbol{\mu}_1 a_0 a_j, a_0^2 a_j; a_j a_0^2; a_i a_h a_k \exp(i\gamma_{ihkj}), \\
 &\quad a_i a_h a_k \exp(i\gamma_{i,-h,k,j}), \mathcal{K})
 \end{aligned} \tag{38}$$

⁽⁸⁾ Other representations (Cartesian or mixed polar-Cartesian) are discussed in [43] and an example will be given below.

where $\mathcal{R}_{hk} := \text{Re}[\mathcal{L}_{hk}]$, $\mathcal{I}_{hk} := \text{Im}[\mathcal{L}_{hk}]$ and the numerical coefficients have been reabsorbed in the operators. In Eqs. (37) and (38) new phase-combinations $\gamma_{ikj} := \vartheta_i + \vartheta_k - \vartheta_j$, $\gamma_{ihkj} := \vartheta_i + \vartheta_h + \vartheta_k - \vartheta_j$, ..., naturally appear in the procedure. They are not all independent, but rather linear combinations of the *independent phase-combinations* [43]

$$\gamma_i := \sum_{j=1}^{N_c} k_{ij} \vartheta_j \quad i=1,2,\dots,R \quad (39)$$

where the coefficients k_{ij} are defined by Eqs. (25). Such variables γ_i are therefore equal in number to the resonance conditions (zero, for nonresonant bifurcations) and only affect the proper resonant terms in the AME.

By differentiating Eqs. (39) with respect to t_1 or t_2 and using Eqs. (37₃) and (38₃), *phase-combination modulation equations* are obtained:

$$\left(\prod_{l \in L_i} a_l \right) d_h \gamma_i = \sum_{j=1}^{N_c} k_{ij} \left(\prod_{l \in L_i, l \neq j} a_l \right) \mathcal{J}_{ij}(\cdot), \quad L_i = \{l \mid k_{il} \neq 0\}, \quad h=1,2 \quad (40)$$

Thus, AME in the unknowns (a_0, a_j, γ_i) are finally obtained by grouping (37_{1,2}) and (40) (with $h=1$) or (38_{1,2}) and (40) (with $h=2$). They are two sets of $N_c + 1 + R = M$ equations in the same number of unknowns, which are called first- and second-order *Reduced Amplitude Modulation Equations* (RAME), respectively. It is worth noting that, to any order, *the RAME are equal in number to the codimension of the bifurcation*.

5.5. Steady-state solutions

First, some properties of the steady-state solutions of the RAME are analyzed. By enforcing $a_0 = \text{const}$, $a_j = \text{const}$, $\gamma_i = \text{const}$, it follows from Eqs. (37₃) and (38₃), that $\vartheta_j = \nu_j t + \varphi_j$, with $\varphi_j = \text{const}$ being the initial phases and $\nu_j = \text{const}$ the *frequency corrections*. Hence, Eq. (39) entails that $\sum_{j=1}^{N_c} k_{ij} \nu_j = 0$ together with $\sum_{j=1}^{N_c} k_{ij} \varphi_j = \gamma_i$; consequently, by using Eq. (25), $\sum_{j=1}^{N_c} k_{ij} \Omega_j = 0$, with $\Omega_j := \omega_j + \nu_j$ being the *nonlinear frequencies*. The nonlinear frequencies Ω_j thus satisfy the resonance conditions in the same way that the linear frequencies ω_j do. If the latter are all in (small) rational ratios (as happens for resonances of the 1:2, 1:3 type), *the motion is periodic*, of short period; otherwise it is a combination of several harmonics (as happens for combination resonances of the $\omega_1 + \omega_2 = \omega_3$ type, or when some critical eigenvalues are not involved in resonances). At the leading order the motion is described by Eq. (30), with $\mathbf{x} = \varepsilon \mathbf{x}_1$ and ε reabsorbed:

$$\mathbf{x}_1 = a_0 \mathbf{u}_0 + \sum_{j=1}^{N_c} a_j \left(\text{Re}[\mathbf{u}_j] \cos(\Omega_j t + \varphi_j) - \text{Im}[\mathbf{u}_j] \sin(\Omega_j t + \varphi_j) \right) \quad (41)$$

where $N_c - R$ of the initial phases φ_j are arbitrary, the remaining being related to the steady values of γ_i ($i=1, \dots, R$).

Steady solutions (a_0, a_j, γ_i) depend on control parameters $\boldsymbol{\mu}$. To evaluate this

dependence, the steady version ($d_h a_0 = d_h a_j = d_h \gamma_i = 0$, $h=1,2$) of the RAME must be solved. The steady first-order equations (37_{1,2}) and (40) and the steady second-order equations (38_{1,2}) and (40) are two sets of algebraic equations that are linear in the first- and second-order parts of the parameter variations $\boldsymbol{\mu}_1$ and $\boldsymbol{\mu}_2$, respectively. Moreover, *the coefficients of $\boldsymbol{\mu}_1$ and $\boldsymbol{\mu}_2$ are equal in the two sets of equations*, since both arise from the terms $\mathbf{F}_{x\boldsymbol{\mu}}^0 \mathbf{x}_1 \boldsymbol{\mu}_1$ and $\mathbf{F}_{x\boldsymbol{\mu}}^0 \mathbf{x}_1 \boldsymbol{\mu}_2$ in the perturbation equations (29₂) and (29₃) respectively. The two steady equations thus have the following structure:

$$\begin{aligned} \mathbf{L}\boldsymbol{\mu}_1 + \mathbf{f}_1(a_0, a_j, \lambda_j) = 0 & \Rightarrow \mathbf{L}\boldsymbol{\mu}_1 + \mathbf{f}_1(a_0, a_j, \gamma_j) = 0 \\ \mathbf{L}\boldsymbol{\mu}_2 + \mathbf{f}_2(a_0, a_j, \lambda_j, \boldsymbol{\mu}_1) = 0 & \Rightarrow \mathbf{L}\boldsymbol{\mu}_2 + \mathbf{f}_2(a_0, a_j, \gamma_j, \boldsymbol{\mu}_1) = 0 \end{aligned} \quad (42)$$

where \mathbf{L} is the $M \times M$ matrix:

$$\mathbf{L} := \begin{bmatrix} a_0 \boldsymbol{\alpha}_{0\boldsymbol{\mu}} \\ a_j \boldsymbol{\alpha}_{j\boldsymbol{\mu}} \\ \left(\prod_{l \in L_i} a_l \right) \sum_j k_{ij} \boldsymbol{\omega}_{j\boldsymbol{\mu}} \end{bmatrix} \quad (43)$$

and

$$\boldsymbol{\alpha}_{0\boldsymbol{\mu}} = \mathbf{v}_0^H \mathbf{F}_{x\boldsymbol{\mu}}^0 \mathbf{u}_0, \quad \boldsymbol{\alpha}_{j\boldsymbol{\mu}} = \text{Re}[\mathbf{v}_j^H \mathbf{F}_{x\boldsymbol{\mu}}^0 \mathbf{u}_j], \quad \boldsymbol{\omega}_{j\boldsymbol{\mu}} = \text{Im}[\mathbf{v}_j^H \mathbf{F}_{x\boldsymbol{\mu}}^0 \mathbf{u}_j] \quad (44)$$

In Eq. (44) $\boldsymbol{\alpha}_{0\boldsymbol{\mu}} := (d\lambda_0/d\boldsymbol{\mu})_0$, $\boldsymbol{\alpha}_{j\boldsymbol{\mu}} + i\boldsymbol{\omega}_{j\boldsymbol{\mu}} := (d\lambda_j/d\boldsymbol{\mu})_0$ are the *real and imaginary parts of the first-order sensitivities of the critical eigenvalues* (see Eqs. (13) and (11₂) with $\mathbf{y}_E \equiv 0$) [14,17,20]. The product $\mathbf{L}\boldsymbol{\mu}_1$ thus assumes the following remarkable geometrical meaning: it represents M hyper-planes which are tangent at the critical manifolds $\lambda_0 = 0$, $\text{Re}\lambda_j = 0$, $\sum_j k_{ij} \text{Im}\lambda_j = 0$ at the critical point. *By assuming that the manifolds are not tangential at this point* (transversality condition), it follows that all the rows of the matrix \mathbf{L} are linearly independent. Therefore Eqs. (42₁) can be solved univocally to furnish the M $\boldsymbol{\mu}_1$ -parameters as functions of the M amplitudes (a_0, a_j, γ_i). By substituting $\boldsymbol{\mu}_1$ in Eq. (42₂), $\boldsymbol{\mu}_2$'s is also expressed as a function of the same amplitudes. By combining $\boldsymbol{\mu}_1$ and $\boldsymbol{\mu}_2$ according to the expansion (26₂), the bifurcation diagram is found in the form $\boldsymbol{\mu} = \boldsymbol{\mu}(a_0, a_j, \gamma_i)$. According the findings of Sect. 2, the procedure shows that *only M parameters are necessary to describe a non-defective bifurcation of codimension- M* . A lower number of parameters would not be sufficient to solve Eqs. (42); a higher number would leave some of them indeterminate.

5.6. Reconstituted bifurcation equations

As already observed, the solvability conditions furnished by the MSM, govern the evolution of the amplitudes on the slow time-scales. They should be solved in sequence to determine the dependence of the amplitudes first on t_1 , then on t_2 , and so on. However, this procedure is inapplicable in the general case, so that an alternative method has to be followed. This consists in combining the solvability equations in a unique equation by

returning to the true time t , using the chain rule (28) [44,45]. Thus, the complex AME (35) and (36) are reconstituted as:

$$\begin{aligned} \dot{a}_0 &= \mathcal{L}_0(\boldsymbol{\mu}a_0, a_0^2; A_l \bar{A}_l; \boldsymbol{\mu}^2 a_0, \boldsymbol{\mu}a_0^2, a_0^3, \boldsymbol{\mu}A_l \bar{A}_l, a_0 A_l \bar{A}_l; A_l A_h A_k, A_l \bar{A}_h A_k, \kappa) \\ \dot{A}_j &= \mathcal{L}_j(\boldsymbol{\mu}A_j, a_0 A_j; A_l A_k, A_l \bar{A}_k; \boldsymbol{\mu}^2 A_j, \boldsymbol{\mu}a_0 A_j, a_0^2 A_j; A_l A_l \bar{A}_l; A_l A_h A_k, A_l \bar{A}_h A_k, \kappa) \quad (45) \\ \forall l, \quad \forall(i, k) |\omega_i \pm \omega_k &= \omega_j, \quad \forall(i, h, k) |\omega_i \pm \omega_h \pm \omega_k = (0, \omega_j) \end{aligned}$$

They are, for example, amenable to a numerical integration, in contrast with the original equations. In Eqs. (45) the bifurcation parameters $\boldsymbol{\mu}$, have also been reconstituted, in addition to the time, according to their series expansion (26₂) and consistently with the order of approximation; moreover the perturbation parameter ε has been reabsorbed according to the rules: $\varepsilon(a_0, A_j) \rightarrow (a_0, A_j)$, $\varepsilon\boldsymbol{\mu}_1 + \varepsilon^2\boldsymbol{\mu}_2 \rightarrow \boldsymbol{\mu}$, $\varepsilon^2\boldsymbol{\mu}_1^2 \rightarrow \boldsymbol{\mu}^2$, $\varepsilon^3\boldsymbol{\mu}_1 a_0^2 \rightarrow \boldsymbol{\mu}a_0^2$ and so on. The reconstituted AME can successively be reduced to their codimension (reconstituted RAME) by introducing phase-combinations; alternatively, reconstitution can be performed directly by combining the first- and second-order RAME.

It should be observed that, if reconstituted AME (or RAME) are to be obtained, *there is no need to expand the bifurcation parameters $\boldsymbol{\mu}$ first*, given that they also have to be reconstituted. In contrast, it is computationally convenient *to order* the bifurcation parameters, rather than *to expand* them. For instance, by letting $\boldsymbol{\mu} = \varepsilon\hat{\boldsymbol{\mu}}$, with $\hat{\boldsymbol{\mu}} = O(1)$, simpler perturbation equations than Eqs. (29) are obtained, in which $\boldsymbol{\mu}_2 \equiv 0$ and $\boldsymbol{\mu}_1 \equiv \hat{\boldsymbol{\mu}}$. Most conveniently, in problems in which the quadratic terms $\mathbf{F}_{xx}^0 x_1^2$ in Eq. (29₂) do not produces resonant terms (see Sect. 7.2 below for an example), it is suitable to order the bifurcation parameters at an higher level, by letting $\boldsymbol{\mu} = \varepsilon^2\hat{\boldsymbol{\mu}}$; in this way perturbation equations in which $\boldsymbol{\mu}_1 = 0$, $\boldsymbol{\mu}_2 \equiv 2\hat{\boldsymbol{\mu}}$ are obtained in place of Eqs. (29). Of course, if the parameters are ordered, rather than expanded, steady solutions cannot be found as previously illustrated, by requiring amplitudes and phase-combinations to be constant on all the time-scales independently, since an insufficient number of parameters would be available; in contrast, stationarity must be enforced on the reconstituted true time-scale t .

The reconstituted AME (or RAME) are asymptotic representation of a *reduced dynamical system* of dimensions equal to the number $2N_c + 1$ of the critical eigenvalues (or to the codimension M), able to capture the main aspects of the original system (22). The MSM can therefore be viewed as a *reduction method*, as for example the Center Manifold Method [13].

5.7. Effects of imperfections

Let us assume now that the system (22) is affected by small imperfections of amplitudes $\boldsymbol{\eta}$. The equations of motion modify as follows:

$$\dot{\mathbf{x}} = \mathbf{F}(\mathbf{x}, \boldsymbol{\mu}, \boldsymbol{\eta}) \quad \mathbf{x} \in \mathbb{R}^N, \boldsymbol{\mu} \in \mathbb{R}^M, \boldsymbol{\eta} \in \mathbb{R}^{C-M} \quad (46)$$

with C being the nonlinear codimension of the bifurcation (see Sect. 2). When the system is perfect ($\boldsymbol{\eta} = \mathbf{0}$) it admits the trivial solution $\mathbf{x} = \mathbf{0} \quad \forall \boldsymbol{\mu}$, i.e. $\mathbf{F}(\mathbf{0}, \boldsymbol{\mu}, \mathbf{0}) \neq \mathbf{0} \quad \forall \boldsymbol{\mu}$; when it is imperfect ($\boldsymbol{\eta} \neq \mathbf{0}$), the trivial solution is no more of equilibrium, i.e. $\mathbf{F}(\mathbf{0}, \boldsymbol{\mu}, \boldsymbol{\eta}) = \mathbf{0}$. A

monoparametric family of solutions to Eq. (46) $\{\mathbf{x} = \mathbf{x}(t, \boldsymbol{\mu}(\varepsilon), \boldsymbol{\eta}(\varepsilon)), \boldsymbol{\mu} = \boldsymbol{\mu}(\varepsilon), \boldsymbol{\eta} = \boldsymbol{\eta}(\varepsilon)\}$ is sought, *by assuming* $\boldsymbol{\eta} \ll \boldsymbol{\mu}$. Therefore, if $\boldsymbol{\mu}$ is expanded according to Eq. (26₂), $\boldsymbol{\eta}$ is ordered as $\boldsymbol{\eta} = \varepsilon^2 \hat{\boldsymbol{\eta}}$, with $\hat{\boldsymbol{\eta}} = O(1)$. Thus, the extra term $\mathbf{F}_{\boldsymbol{\eta}}^0 \hat{\boldsymbol{\eta}}$ appears in the perturbation equation (29₂) and further terms $\mathbf{F}_{\boldsymbol{\mu}\boldsymbol{\eta}}^0 \boldsymbol{\mu}_1 \hat{\boldsymbol{\eta}}$, $\mathbf{F}_{\boldsymbol{\eta}\boldsymbol{x}_1}^0 \boldsymbol{x}_1 \hat{\boldsymbol{\eta}}$ in Eq. (29₃). These in turn entail a known term proportional to $\hat{\boldsymbol{\eta}}$ entering Eqs. (35) and new terms proportional to $\boldsymbol{\mu}_1 \hat{\boldsymbol{\eta}}$ and $(a_0 \hat{\boldsymbol{\eta}}, A_j \hat{\boldsymbol{\eta}})$ entering Eqs. (36). It should be noted that $\mathbf{F}_{\boldsymbol{\eta}}^0 \hat{\boldsymbol{\eta}}$ destroys the trivial solution $(a_0, A_j) = (0, 0)$ if and only if its projections onto the critical modes, $\mathbf{v}_0^H \mathbf{F}_{\boldsymbol{\eta}}^0 \hat{\boldsymbol{\eta}}$ and $\mathbf{v}_j^H \mathbf{F}_{\boldsymbol{\eta}}^0 \hat{\boldsymbol{\eta}}$ are not all zero. Indeed, if $\mathbf{F}_{\boldsymbol{\eta}}^0 \hat{\boldsymbol{\eta}}$ is orthogonal to the eigenspace, then it is filtered by the projection (32) and does not enter the AME. In this case although $\boldsymbol{\eta}$ destroys the trivial fundamental path, it is not an imperfection for the bifurcation under analysis, since it only affects (at the first-order) the noncritical components of motion.

Once imperfections have been taken into account, bifurcation diagrams in form $\boldsymbol{\mu} = \boldsymbol{\mu}(a_0, a_j, \gamma_i; \boldsymbol{\eta})$ are found. If the bifurcation parameters are ordered, rather than expanded, $\boldsymbol{\eta} = \varepsilon^2 \hat{\boldsymbol{\eta}}$ must be taken if $\boldsymbol{\mu} = \varepsilon \hat{\boldsymbol{\mu}}$, and $\boldsymbol{\eta} = \varepsilon^3 \hat{\boldsymbol{\eta}}$ if $\boldsymbol{\mu} = \varepsilon^2 \hat{\boldsymbol{\mu}}$.

6. Multiple scale method for defective bifurcations

Let us assume that at the bifurcation point O the Jacobian $\mathbf{F}_{\mathbf{x}}^0$ admits at least one critical eigenvalue λ_{0j} with algebraic multiplicity $m > 1$. In the generic case, only one critical eigenvector \mathbf{u}_j is associated with λ_{0j} , so that the matrix $\mathbf{F}_{\mathbf{x}}^0$ has an incomplete set of eigenvectors (it is defective, or nilpotent). If the algorithm for non-defective bifurcations is applied here, a drawback similar to that encountered in sensitivity analysis (Sect. 4.2) will arise. Indeed, because \mathbf{u}_j is orthogonal to the (unique) left eigenvector \mathbf{v}_j , when solvability conditions are enforced to the ε^2 -order perturbation equation (29₂), the coefficient of the relevant amplitude derivative in Eqs. (32) vanishes and the procedure fails.

On the other hand the bifurcation analysis is formally similar to sensitivity analysis. Indeed, if the equations of motion are expanded and written in the form:

$$[\mathbf{F}_{\mathbf{x}}^0 + \varepsilon(1/2 \mathbf{F}_{\mathbf{x}\mathbf{x}}^0 \hat{\mathbf{x}} + \dots) - D] \hat{\mathbf{x}} = \mathbf{0} \quad (47)$$

where the change of variable $\mathbf{x} \rightarrow \varepsilon \hat{\mathbf{x}}$ has been introduced and $D = d/dt$ has been posed, then Eq. (47) is formally equal to the perturbed eigenvalue problem $(\mathbf{A}_0 + \varepsilon \mathbf{A}_1 + \dots - \lambda) \mathbf{w} = \mathbf{0}$ in which λ is substituted by the operator D . The analogy suggests the expedience of introducing *fractional power expansion of $\varepsilon^{1/m}$* for both the ‘eigenvector’ \mathbf{x} and the ‘eigenvalue’ D , namely:

$$\begin{aligned} \mathbf{x} &= \varepsilon(\mathbf{x}_0 + \varepsilon^{1/m} \mathbf{x}_1 + \varepsilon^{2/m} \mathbf{x}_2 + \dots) \\ \frac{d}{dt} &= d_0 + \varepsilon^{1/m} d_1 + \varepsilon^{2/m} d_2 + \dots \end{aligned} \quad (48)$$

where a return to \mathbf{x} is made. The formal series expansion of d/dt corresponds to the introduction of the following *fractional time-scales*:

$$t_0 = t, \quad t_1 = \varepsilon^{1/m} t, \quad t_2 = \varepsilon^{2/m} t, \dots \quad (49)$$

with $d_k := \partial/\partial t_k$ ($k = 1, 2, \dots$). It will be proved, that the series expansion (48) works well when \mathbf{F}_x^0 possesses a unique critical eigenvalue of algebraic multiplicity $m > 1$ and geometrical multiplicity 1. More complex cases, such as the simultaneous occurrence of other non-defective, as well as defective, eigenvalues have not been studied so far; however, it is believed that sensitivity analysis can again be helpful in suggesting strategies for their solution.

Let us therefore assume that \mathbf{F}_x^0 has the unique critical eigenvalue $\lambda_0 = 0$ (defective divergence) or the unique couple of critical eigenvalues $\lambda_0 = \pm i\omega$ (defective Hopf), in both cases of algebraic multiplicity $m > 1$ (bifurcation of codimension m or $2m - 1$, respectively). Let $\{\mathbf{u}_1, \mathbf{u}_2, \dots, \mathbf{u}_m\}$ be the chain of the associated (right) generalized eigenvectors satisfying Eqs. (14) (index j omitted), and \mathbf{v}_m the unique proper left eigenvector. The two bifurcations are discussed separately.

6.1. Defective divergence

The series expansions (48) are adopted; in addition, the bifurcation parameters are scaled as $\boldsymbol{\mu} = \varepsilon \hat{\boldsymbol{\mu}}$, in order that the lowest-order derivative $\mathbf{F}_{\boldsymbol{\mu}}^0 \mathbf{x}_0 \hat{\boldsymbol{\mu}}$ appears at the same level of the resonant term $\mathbf{F}_{\mathbf{x}\mathbf{x}}^0 \mathbf{x}_0^2$. The following perturbation equations are drawn:

$$\begin{aligned} \varepsilon: & (d_0 - \mathbf{F}_x^0) \mathbf{x}_0 = 0 \\ \varepsilon^{1+1/m}: & (d_0 - \mathbf{F}_x^0) \mathbf{x}_1 = d_1 \mathbf{x}_0 \\ \varepsilon^{1+2/m}: & (d_0 - \mathbf{F}_x^0) \mathbf{x}_2 = d_1 \mathbf{x}_1 + d_2 \mathbf{x}_0 \\ & \dots\dots\dots \\ \varepsilon^2: & (d_0 - \mathbf{F}_x^0) \mathbf{x}_m = d_1 \mathbf{x}_{m-1} + d_2 \mathbf{x}_{m-2} + \kappa + 1/2 \mathbf{F}_{\mathbf{x}\mathbf{x}}^0 \mathbf{x}_0^2 + \mathbf{F}_{\boldsymbol{\mu}}^0 \mathbf{x}_0 \hat{\boldsymbol{\mu}} \\ \varepsilon^{2+1/m}: & (d_0 - \mathbf{F}_x^0) \mathbf{x}_{m+1} = d_1 \mathbf{x}_m + d_2 \mathbf{x}_{m-1} + \kappa + \mathbf{F}_{\mathbf{x}\mathbf{x}}^0 \mathbf{x}_0 \mathbf{x}_1 + \mathbf{F}_{\boldsymbol{\mu}}^0 \mathbf{x}_1 \hat{\boldsymbol{\mu}} \end{aligned} \quad (50)$$

Since a unique real critical eigenvector exists, the non-diverging and not damped (on the fast scale) solution to Eq. (50₁) is:

$$\mathbf{x}_0 = a(t_1, t_2, \dots) \mathbf{u}_1 \quad (51)$$

where a is the unknown time-dependent real amplitude. The perturbation equations of order lower than ε^2 can be solved without requiring any solvability conditions, since their known terms all belong to the range of the operator. It follows that $\mathbf{x}_1 = d_1 a \mathbf{u}_2$, $\mathbf{x}_2 = d_1^2 a \mathbf{u}_3 + d_2 a \mathbf{u}_1$, ..., $\mathbf{x}_{m-1} = d_1^{m-1} a \mathbf{u}_m + \dots$. Therefore, at the ε^2 -order, terms $d_1^m a \mathbf{u}_m$ and $d_2 d_1^{m-2} a \mathbf{u}_{m-1}$ appear in the equation, together with $\mathbf{F}_{\mathbf{x}\mathbf{x}}^0 \mathbf{x}_0^2$ and $\mathbf{F}_{\boldsymbol{\mu}}^0 \mathbf{x}_0 \hat{\boldsymbol{\mu}}$, which are proportional to a^2 and $a \hat{\boldsymbol{\mu}}$, respectively. By enforcing solvability, a differential equation of order m is drawn, of the type:

$$d_1^m a = \mathcal{L}_m(a \hat{\boldsymbol{\mu}}, a^2) \quad (52)$$

By solving the ε^2 -order equation, \mathbf{x}_m is found. It contains the term $d_2 d_1^{m-2} a \mathbf{u}_m$ which, at the $\varepsilon^{2+1/m}$ -order, enters the solvability condition, which therefore reads:

$$m d_2 d_1^{m-1} a = \mathcal{L}_{m+1}(\hat{\boldsymbol{\mu}} d_1 a, a d_1 a) \quad (53)$$

since $\mathbf{F}_{\mathbf{x}\mathbf{x}}^0 \mathbf{x}_0 \mathbf{x}_1$ and $\mathbf{F}_{\mathbf{x}\boldsymbol{\mu}}^0 \mathbf{x}_1 \hat{\boldsymbol{\mu}}$ are proportional to $a d_1 a$ and $\hat{\boldsymbol{\mu}} d_1 a$, respectively. By proceeding to higher orders, other solvability conditions involving combinations of derivatives such as $m d_3 d_1^{m-1} a + m(m-1)/2 d_2^2 d_1^{m-2} a$ are found, *i.e. terms of the m -th derivative of a* :

$$\frac{d^m a}{dt^m} = \varepsilon [d_1^m + m \varepsilon^{1/m} d_1^{m-1} d_2 + \varepsilon^{2/m} (m d_1^{m-1} d_3 + \frac{1}{2} m(m-1) d_1^{m-2} d_2^2) + \mathbf{K}] a \quad (54)$$

Therefore, by combining all the solvability conditions in a unique equation, a reconstituted bifurcation equation is drawn, comprising a differential equation of the m -th order:

$$D^m a = \mathcal{L}(a \boldsymbol{\mu}, a^2; \dot{a} \boldsymbol{\mu}, a \dot{a}; \ddot{a} \boldsymbol{\mu}, a \ddot{a}, \dot{a}^2; \dots) \quad (55)$$

where the parameter ε has been reabsorbed according to the rules $\varepsilon a \rightarrow a$, $\varepsilon \hat{\boldsymbol{\mu}} \rightarrow \boldsymbol{\mu}$, and $\varepsilon^{1/m} d/dt \rightarrow d/dt$. In Eq. (53) $D^m a$ is a term of the ε^2 -order, while the right hand member contains (separated by semicolons) all the terms of the order ε^2 ; $\varepsilon^{2+1/m}$, $\varepsilon^{2+2/m}$, ..., up to the highest order accounted for in the analysis. For example, if $m = 3$, the bifurcation equation at the ε^3 -order reads:

$$\ddot{a} = \mathcal{L}(a \boldsymbol{\mu}, a^2; \dot{a} \boldsymbol{\mu}, a \dot{a}; \ddot{a} \boldsymbol{\mu}, a \ddot{a}, \dot{a}^2; \boldsymbol{\mu}^3, a^2 \boldsymbol{\mu}, a^3, a \ddot{a}) \quad (56)$$

while at the $\varepsilon^{10/3}$ -order (*i.e.* one step further) it becomes:

$$\ddot{a} = \mathcal{L}(\dots; \dot{a} \boldsymbol{\mu}^2, a^2 \dot{a}, a \dot{a} \boldsymbol{\mu}, \dot{a}^2) \quad (57)$$

where only additional terms have been displayed^(§).

6.2. Defective Hopf bifurcation

The success of the series expansion (48) depends on the higher-order generalized eigenvector \mathbf{u}_m appearing in the ε^2 -order perturbation equations, *i.e.* at the same level of the resonant perturbation $\mathbf{F}_{\mathbf{x}\mathbf{x}}^0 \mathbf{x}_0^2$. However, when a Hopf bifurcation is considered for which \mathbf{x}_0 is a harmonic function of time, *this quadratic term is not resonant*, since it is the sum of a double harmonic and a constant term. In contrast, resonance is produced by the cubic nonlinearity $\mathbf{F}_{\mathbf{x}\mathbf{x}\mathbf{x}}^0 \mathbf{x}_0^3$, at the ε^3 -order. This case is similar to that occurring in sensitivity analysis, when the perturbation $\mathbf{v}_m^H \mathbf{A}_1 \mathbf{u}_1$ is of the order ε^2 (or zero) instead of the order ε (as supposed in the generic case, see Eq. (18)), thus entailing $\Delta \lambda = O(\varepsilon^{2/m})$.

^(§) The derivatives of a in the r. h. m. of Eq. (55) are however of orders lower than m , since use of Eqs. (52), (53), ... has been made. For example $d_1^{m+1} a$ can be written as $d_1(\mathbf{L}_m(a \hat{\boldsymbol{\mu}}, a^2))$. This point should be compared with the discussion made at the end of Sect. 4 about reconstituted sensitivity equations.

The analogy suggests expanding the time-derivative operator D in series of fractional powers of $\varepsilon^{2/m}$ rather than $\varepsilon^{1/m}$ or, equivalently, omitting the ‘odd’ powers $\varepsilon^{(2k+1)/m}$ in the expansion (48). Similarly, the same expansion should be taken for the state variable \mathbf{x} . However, a new problem then arises. Indeed, if m is odd, series expansions of $\varepsilon^{2k/m}$ do not contain the power 1 so that no ε^2 -order perturbation equations would appear in which to place $\mathbf{F}_{\mathbf{x}\mathbf{x}}^0 \mathbf{x}_0^2$. In contrast, the drawback does not occur if m is even. It is therefore conjectured that *a complete series of $\varepsilon^{1/m}$ must be considered for \mathbf{x} if m is odd, while only the even powers must be taken if m is even*⁽⁸⁾. In both cases the scaling $\hat{\boldsymbol{\mu}} = \varepsilon^2 \hat{\boldsymbol{\mu}}$ must be introduced to render $\mathbf{F}_{\mathbf{x}\hat{\boldsymbol{\mu}}}^0 \mathbf{x}_0 \hat{\boldsymbol{\mu}}$ of the same order as the resonant term $\mathbf{F}_{\mathbf{x}\mathbf{x}\mathbf{x}}^0 \mathbf{x}_0^3$. The two cases are now analyzed and the validity of the conjecture proved.

6.2.1. Even m case

By omitting the odd powers of $\varepsilon^{1/m}$ in the series (48) and using $\boldsymbol{\mu} = \varepsilon^2 \hat{\boldsymbol{\mu}}$, the following perturbation equations are obtained:

$$\begin{aligned}
 \varepsilon: (d_0 - \mathbf{F}_{\mathbf{x}}^0) \mathbf{x}_0 &= 0 \\
 \varepsilon^{1+2/m}: (d_0 - \mathbf{F}_{\mathbf{x}}^0) \mathbf{x}_2 &= d_2 \mathbf{x}_0 \\
 \varepsilon^{1+4/m}: (d_0 - \mathbf{F}_{\mathbf{x}}^0) \mathbf{x}_4 &= d_2 \mathbf{x}_2 + d_4 \mathbf{x}_0 \\
 &\dots\dots\dots \\
 \varepsilon^2: (d_0 - \mathbf{F}_{\mathbf{x}}^0) \mathbf{x}_m &= d_2 \mathbf{x}_{m-2} + d_4 \mathbf{x}_{m-4} + \kappa + 1/2 \mathbf{F}_{\mathbf{x}\mathbf{x}}^0 \mathbf{x}_0^2 \\
 \varepsilon^{2+2/m}: (d_0 - \mathbf{F}_{\mathbf{x}}^0) \mathbf{x}_{m+2} &= d_2 \mathbf{x}_m + d_4 \mathbf{x}_{m-2} + \kappa + \mathbf{F}_{\mathbf{x}\mathbf{x}}^0 \mathbf{x}_0 \mathbf{x}_2 \\
 &\dots\dots\dots \\
 \varepsilon^3: (d_0 - \mathbf{F}_{\mathbf{x}}^0) \mathbf{x}_{2m} &= d_2 \mathbf{x}_{2m-2} + d_4 \mathbf{x}_{2m-4} + \kappa + 1/6 \mathbf{F}_{\mathbf{x}\mathbf{x}\mathbf{x}}^0 \mathbf{x}_0^3 \\
 &\quad + \mathbf{F}_{\mathbf{x}\mathbf{x}}^0 (\mathbf{x}_0 \mathbf{x}_m + \mathbf{x}_2 \mathbf{x}_{m-2} + \kappa) + \mathbf{F}_{\mathbf{x}\hat{\boldsymbol{\mu}}}^0 \mathbf{x}_0 \hat{\boldsymbol{\mu}} \\
 \varepsilon^{3+2/m}: (d_0 - \mathbf{F}_{\mathbf{x}}^0) \mathbf{x}_{2m+2} &= d_2 \mathbf{x}_{2m} + d_4 \mathbf{x}_{2m-2} + \kappa + 1/2 \mathbf{F}_{\mathbf{x}\mathbf{x}\mathbf{x}}^0 \mathbf{x}_0^2 \mathbf{x}_2 \\
 &\quad + \mathbf{F}_{\mathbf{x}\mathbf{x}}^0 (\mathbf{x}_0 \mathbf{x}_{m+2} + \mathbf{x}_2 \mathbf{x}_m + \kappa) + \mathbf{F}_{\mathbf{x}\hat{\boldsymbol{\mu}}}^0 \mathbf{x}_2 \hat{\boldsymbol{\mu}}
 \end{aligned} \tag{58}$$

The ε -order perturbation equation admits the generating solution:

$$\mathbf{x}_0 = A(t_2, t_4, \dots) \mathbf{u}_1 e^{i\omega t_0} + c.c. \tag{59}$$

in which A is the unknown time-dependent complex amplitude. By proceeding, the equations can be solved up to the ε^3 -order without requiring solvability, since the resonant terms all belong to the range of the operator. In particular, $\mathbf{x}_2, \mathbf{x}_4, \dots, \mathbf{x}_{m-2}$ only contain the simple harmonic ω , while $\mathbf{x}_m, \mathbf{x}_{m+2}, \dots, \mathbf{x}_{2m-2}$ also contain the double harmonic 2ω and the constant term generated by the quadratic nonlinearities. When the ε^3 -order equation is reached, the resonant terms finally appear, produced by the cubic nonlinearities $\mathbf{F}_{\mathbf{x}\mathbf{x}\mathbf{x}}^0 \mathbf{x}_0^3$ as well as by the quadratic nonlinearities $\mathbf{F}_{\mathbf{x}\mathbf{x}}^0 \mathbf{x}_0 \mathbf{x}_m$, in addition to the parameter-dependent term $\mathbf{F}_{\mathbf{x}\hat{\boldsymbol{\mu}}}^0 \mathbf{x}_0 \hat{\boldsymbol{\mu}}$. These resonant terms, which are proportional to $A^2 \bar{A}$ and $A \hat{\boldsymbol{\mu}}$, all enter the first solvability condition, together with the derivative $d_2^m A$ which multiplies the higher

⁽⁸⁾ It should be noticed that, if $m = 2$, only integer powers of ε exist, as a special case.

eigenvector of the chain \mathbf{u}_m . The condition thus reads:

$$d_2^m A = \mathcal{L}_m(A\hat{\boldsymbol{\mu}}, A^2\bar{A}) \quad (60)$$

At the higher-order levels, solvability conditions such as:

$$m d_4 d_2^{m-1} A = \mathcal{L}_{m+1}(\hat{\boldsymbol{\mu}} d_2 A, A\bar{A} d_2 A, A^2 d_2 \bar{A}) \quad (61)$$

are obtained, from which the following reconstituted bifurcation equation is drawn:

$$D^m A = \mathcal{L}(\boldsymbol{\mu} A, A^2 \bar{A}; \boldsymbol{\mu} \dot{A}, A\bar{A}\dot{A}, A^2 \ddot{A}; \dots) \quad (62)$$

in which the parameter ε has been reabsorbed according to the rules $\varepsilon A \rightarrow A$, $\varepsilon^2 \hat{\boldsymbol{\mu}} \rightarrow \boldsymbol{\mu}$, and $\varepsilon^{2/m} d/dt \rightarrow d/dt$. In Eq. (60) $D^m A$ is a term of the ε^3 -order, while the right hand member contains (separated by semicolons) all terms associated with frequency ω of the order ε^3 , $\varepsilon^{3+2/m}$, ..., up to the highest order accounted for in the analysis⁽⁶⁾. For example, if $m = 4$, the bifurcation equation at the ε^4 -order reads:

$$A = \mathcal{L}(\boldsymbol{\mu} A, A^2 \bar{A}; \boldsymbol{\mu} \dot{A}, A\bar{A}\dot{A}, A^2 \ddot{A}; \boldsymbol{\mu} \ddot{A}, \dot{A}^2 \bar{A}, A\dot{A}\ddot{A}) \quad (63)$$

6.2.2 Odd m case

By omitting the odd powers of $\varepsilon^{1/m}$ in the series (48₂), but keeping them in the series (48₁) and using the ordering $\boldsymbol{\mu} = \varepsilon^2 \hat{\boldsymbol{\mu}}$, the following perturbation equations are obtained:

$$\begin{aligned} \varepsilon : (d_0 - \mathbf{F}_x^0) \mathbf{x}_0 &= 0 \\ \varepsilon^{1+1/m} : (d_0 - \mathbf{F}_x^0) \mathbf{x}_1 &= 0 \\ \varepsilon^{1+2/m} : (d_0 - \mathbf{F}_x^0) \mathbf{x}_2 &= d_2 \mathbf{x}_0 \\ \varepsilon^{1+3/m} : (d_0 - \mathbf{F}_x^0) \mathbf{x}_3 &= d_2 \mathbf{x}_1 \\ \varepsilon^{1+4/m} : (d_0 - \mathbf{F}_x^0) \mathbf{x}_4 &= d_2 \mathbf{x}_2 + d_4 \mathbf{x}_0 \\ &\dots\dots\dots \\ \varepsilon^2 : (d_0 - \mathbf{F}_x^0) \mathbf{x}_m &= d_2 \mathbf{x}_{m-2} + d_4 \mathbf{x}_{m-4} + \dots + 1/2 \mathbf{F}_{xx}^0 \mathbf{x}_0^2 \\ &\dots\dots\dots \\ \varepsilon^3 : (d_0 - \mathbf{F}_x^0) \mathbf{x}_{2m} &= d_2 \mathbf{x}_{2m-2} + d_4 \mathbf{x}_{2m-4} + \dots + 1/6 \mathbf{F}_{xxx}^0 \mathbf{x}_0^3 \\ &\quad + \mathbf{F}_{xx}^0 (\mathbf{x}_0 \mathbf{x}_m + \mathbf{x}_1 \mathbf{x}_{m-1} + \dots) + \mathbf{F}_{xu}^0 \mathbf{x}_0 \hat{\boldsymbol{\mu}} \\ \varepsilon^{3+1/m} : (d_0 - \mathbf{F}_x^0) \mathbf{x}_{2m+1} &= d_2 \mathbf{x}_{2m-1} + d_4 \mathbf{x}_{2m-3} + \dots + 1/2 \mathbf{F}_{xxx}^0 \mathbf{x}_0^2 \mathbf{x}_1 \\ &\quad + \mathbf{F}_{xx}^0 (\mathbf{x}_0 \mathbf{x}_{m+1} + \mathbf{x}_1 \mathbf{x}_m + \dots) + \mathbf{F}_{xu}^0 \mathbf{x}_1 \hat{\boldsymbol{\mu}} \\ \varepsilon^{3+2/m} : (d_0 - \mathbf{F}_x^0) \mathbf{x}_{2m+2} &= d_2 \mathbf{x}_{2m} + d_4 \mathbf{x}_{2m-2} + \dots + \mathbf{F}_{xu}^0 \mathbf{x}_2 \hat{\boldsymbol{\mu}} + 1/2 \mathbf{F}_{xxx}^0 (\mathbf{x}_0^2 \mathbf{x}_2 + \mathbf{x}_0 \mathbf{x}_1^2) \\ &\quad + \mathbf{F}_{xx}^0 (\mathbf{x}_0 \mathbf{x}_{m+2} + \mathbf{x}_1 \mathbf{x}_{m+1} + \dots) a \end{aligned} \quad (64)$$

⁽⁶⁾ Arguments similar to that discussed about Eq. (55) hold.

Since \mathbf{x}_0 is still given by Eq. (59), $\mathbf{x}_2, \mathbf{x}_4, \dots, \mathbf{x}_{2m-2}$ remain unchanged with respect to the previous case; in particular they only contain the fundamental harmonic. Moreover, since $\mathbf{x}_1 = \mathbf{0}$, $\mathbf{x}_3, \mathbf{x}_5, \dots, \mathbf{x}_{m-1}$ also vanish, while $\mathbf{x}_m, \mathbf{x}_{m+2}, \dots, \mathbf{x}_{2m-1}$ are sums of double- and zero-harmonics. Therefore the even terms of the series $\mathbf{x}_0, \mathbf{x}_2, \dots, \mathbf{x}_{2m}, \mathbf{x}_{2m+2}, \dots$, are identical to that of Eqs. (58). When the ε^3 -perturbation equation is considered, resonant terms appear through the same mechanism illustrated above, leading to a solvability condition identical to Eq. (60). At the subsequent orders *no resonant terms appear in the equations in the odd terms*. Indeed, quadratic nonlinearities involve products $\mathbf{x}_i \mathbf{x}_j$, in which (i, j) are either even or odd and therefore of even resultant frequencies; similarly, cubic nonlinearities involve products $\mathbf{x}_i \mathbf{x}_j \mathbf{x}_k$ in which (i, j, k) are either all odd or two even and one odd and therefore still of even frequencies. Therefore, solvability must be required only for the equations in the even terms \mathbf{x}_{2k} , which are still of type (61). Reconstituted bifurcation equations in the form (62) are thus obtained, both for even and odd multiplicities m .

7. Examples of low-codimension bifurcation analysis

Using the techniques of analysis illustrated in Sections 5 and 6 for non-defective and defective bifurcations, respectively, some codimension-2 and codimension-3 bifurcations are studied and some relevant results briefly commented.

7.1. Hopf-divergence bifurcation

In this case the motion is described at the leading order by Eq. (30) in which $N_c = 1$, i.e.

$$\mathbf{x} = \frac{1}{2} a_0 \mathbf{u}_0 + A_1 \mathbf{u}_1 e^{i\omega t} + c.c. \quad (65)$$

with a_0 and A_1 being time-dependent amplitudes. Since no resonances exist, the reconstituted AME (45) read:

$$\dot{a}_0 = \mathcal{L}_0(\boldsymbol{\mu} a_0, a_0^2; A_1 \bar{A}_1; \boldsymbol{\mu}^2 a_0, \boldsymbol{\mu} a_0^2, a_0^3, \boldsymbol{\mu} A_1 \bar{A}_1, a_0 A_1 \bar{A}_1) \quad (66)$$

$$\dot{A}_1 = \mathcal{L}_1(\boldsymbol{\mu} A_1, a_0 A_1; \boldsymbol{\mu}^2 A_1, \boldsymbol{\mu} a_0 A_1, a_0^2 A_1; A_1^2 \bar{A}_1)$$

with $\boldsymbol{\mu} \in \mathbb{R}^2$. By accounting for $a = O(\varepsilon)$, $A_1 = O(\varepsilon)$, $\boldsymbol{\mu} = O(\varepsilon)$, $d/dt = O(\varepsilon)$, Eqs. (66) contains all terms of the orders ε^2 and ε^3 associated with the zero- or ω -frequencies. By adopting the polar representation $A_1 = 1/2 a_1 e^{i\theta_1}$, two differential equations in the real amplitudes a_0 and a_1 are obtained, uncoupled from a third equation, which governs the phase-modulation:

$$\dot{a}_0 = \mathcal{L}_0(\boldsymbol{\mu} a_0, a_0^2; a_1^2; \boldsymbol{\mu}^2 a_0, \boldsymbol{\mu} a_0^2, a_0^3, \boldsymbol{\mu} a_1^2, a_0 a_1^2) \quad (67)$$

$$\dot{a}_1 = \mathcal{L}_1(\boldsymbol{\mu} a_1, a_0 a_1; \boldsymbol{\mu}^2 a_1, \boldsymbol{\mu} a_0 a_1, a_0^2 a_1; a_1^3)$$

Equations (67) are further simplified if the system is symmetric, i.e. if $\mathbf{F}(-\mathbf{x}, \boldsymbol{\mu}) = -\mathbf{F}(\mathbf{x}, \boldsymbol{\mu}) \forall \boldsymbol{\mu}$, for which no quadratic nonlinearities exist, i.e. $\mathbf{F}_{xx}^0 \mathbf{x}^2 \equiv \mathbf{0} \forall \mathbf{x}$. Such a special case is frequently encountered in structural analysis; one example is the system in Fig. 2d. By ordering $\boldsymbol{\mu}$ at the ε^2 -order and also considering the effects of imperfections $\boldsymbol{\eta} = O(\varepsilon^3)$, the relevant bifurcation equations become:

$$\begin{aligned} \dot{a}_0 &= \mathcal{L}_0(\boldsymbol{\mu}a_0, a_0^3, a_0a_1^2; \boldsymbol{\eta}) \\ \dot{a}_1 &= \mathcal{R}_1(\boldsymbol{\mu}a_1, a_0^2a_1; a_1^3) \end{aligned} \quad (68)$$

which only account for the ε^3 -order terms. If $\boldsymbol{\eta} = \mathbf{0}$, Eqs. (68) are invariant under the transformation $a_0 \rightarrow -a_0$ and $a_1 \rightarrow -a_1$; if $\boldsymbol{\eta} \neq \mathbf{0}$ the symmetry with respect to a_0 is destroyed. Equations (68) have been employed in [20] to analyze the post-critical behavior of the system in Fig. 2d, by accounting for both geometrical and aerodynamic nonlinearities. The complete scenario for the perfect system is illustrated on the $(\boldsymbol{\mu}, \nu)$ -plane (Fig. 7a, that should be compared with the linear stability diagram in Fig. 4). Crossing the boundary lines \mathcal{D}_T and \mathcal{H}_T cause divergence and Hopf bifurcation of the trivial solution, giving rise to a new stable equilibrium point E_1 or a periodic motion (limit cycle) P_1 , respectively. Along the new boundary \mathcal{D}_P , the periodic motion P_1 undergoes divergence, losing stability and giving rise to a new stable periodic motion P_2 . To sum up, stable periodic motions exist in regions 2 (around the trivial equilibrium position), 3 and 4 (around the buckled equilibrium position); a stable equilibrium exists in region 5. If imperfections are considered (Fig. 7b), one equilibrium solution exists for $\nu < 0$ and three solutions for $\nu > 0$ (since ν and $\boldsymbol{\eta}$ cause an imperfect fork bifurcation). In regions 2, 3 and 4 stable periodic motions exist around non-trivial equilibria. On account of the interaction, a stable periodic motion P_3 exists in region 3 for $a_0 < 0$, although no equilibrium solutions exists for $a_0 < 0$, for either perfect or imperfect structures.

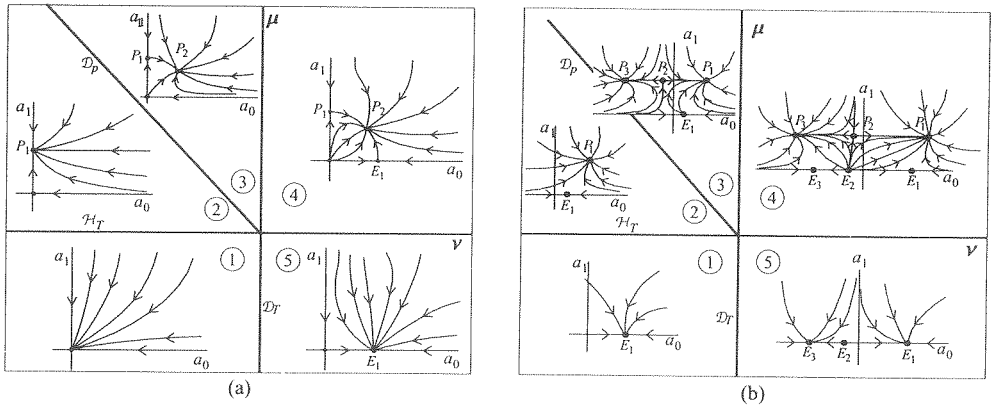


Figure 7. Bifurcation diagram for the structure in Fig. 2d: (a) perfect system ($\boldsymbol{\eta} = \mathbf{0}$), (b) imperfect system ($\boldsymbol{\eta} \neq \mathbf{0}$).

7.2. Nonresonant double-Hopf bifurcation

In this bifurcation $N_c = 2$ complex critical eigenvalues and no zero eigenvalues are involved. For Eq. (30) the motion is:

$$\mathbf{x}_1 = A_1 \mathbf{u}_1 e^{i\omega_1 t_0} + A_2 \mathbf{u}_2 e^{i\omega_2 t_0} + c.c. \quad (69)$$

with A_1 and A_2 being time-dependent complex amplitudes. Since in the perturbation equation (29₂) the quadratic term $\mathbf{F}_{\mathbf{x}\mathbf{x}}^0 \mathbf{x}_1^2$ is not resonant, it is convenient to order $\boldsymbol{\mu} \in \mathbb{R}^2$ as $\boldsymbol{\mu} = \varepsilon^2 \hat{\boldsymbol{\mu}}$; consequently A_1 and A_2 are independent of t_1 . By proceeding to higher orders it is easy to check that *only the even powers of ε of d/dt (Eq. (28)) are different from zero*. By truncating the analysis at the ε^2 -order, i.e. at the first significant level, the following bifurcation equations are drawn:

$$\begin{aligned} \dot{A}_1 &= \mathcal{L}_1(\boldsymbol{\mu} A_1, A_1^2 \bar{A}_1, A_1 A_2 \bar{A}_2) \\ \dot{A}_2 &= \mathcal{L}_2(\boldsymbol{\mu} A_2, A_2 A_1 \bar{A}_1, A_2^2 \bar{A}_2) \end{aligned} \quad (70)$$

These can be considered as being derived from Eq. (45₂) by taking $a_0 = 0$ and omitting the proper resonant terms and the higher powers of $\boldsymbol{\mu}$. By using the polar representation $A_j = 1/2 a_j e^{i\vartheta_j}$, two bifurcation equations in a_1 and a_2 , uncoupled from phase-equations, are drawn:

$$\begin{aligned} \dot{a}_1 &= \mathcal{R}_1(\boldsymbol{\mu} a_1, a_1^3, a_1 a_2^2) \\ \dot{a}_2 &= \mathcal{R}_2(\boldsymbol{\mu} a_2, a_1^2 a_2, a_2^3) \end{aligned} \quad (71)$$

which are invariant under the transformations $a_1 \rightarrow -a_1$, $a_2 \rightarrow -a_2$. Equations (71) have been employed in [17] to analyze the post-critical behavior of the nonresonant system in Fig. 2e, by accounting for both geometrical and aerodynamic nonlinearities. The complete scenario is displayed on the $(\boldsymbol{\mu}, \xi_e)$ -parameter plane (Fig. 8, that should be compared with the linear stability diagram in Fig. 5). At the Hopf boundaries \mathcal{H}_1 and \mathcal{H}_2 two stable periodic motions P_1 and P_2 arise. These lose stability at the Q_1 and Q_2 lines, respectively, where, after a Neimark bifurcation, a quasi-periodic motion Q arises, in which both the modes involved contribute to the motion, each with its own frequency (slightly modified by nonlinearities). To sum up, the structure oscillates in a stable antisymmetric (symmetric) mode in regions 2 and 3 (6 and 5) and in a quasi-periodic motion in region 4.

7.3. 1:2 and 1:3 resonant double-Hopf bifurcations

In these bifurcations Eq. (69) still holds, but with the frequency ratio ω_2/ω_1 equal to 2 or 3.

The 1:3 resonance is easier to be analyzed, since quadratic nonlinearities $\mathbf{F}_{\mathbf{x}\mathbf{x}}^0 \mathbf{x}_1^2$ do not produce resonant terms, and a perturbation scheme identical to the nonresonant case can therefore be adopted. Thus, by ordering $\boldsymbol{\mu} \in \mathbb{R}^3$ as $\boldsymbol{\mu} = \varepsilon^2 \hat{\boldsymbol{\mu}}$ and omitting the even powers of ε in the expansion (28) of d/dt , the bifurcation equations are found at the

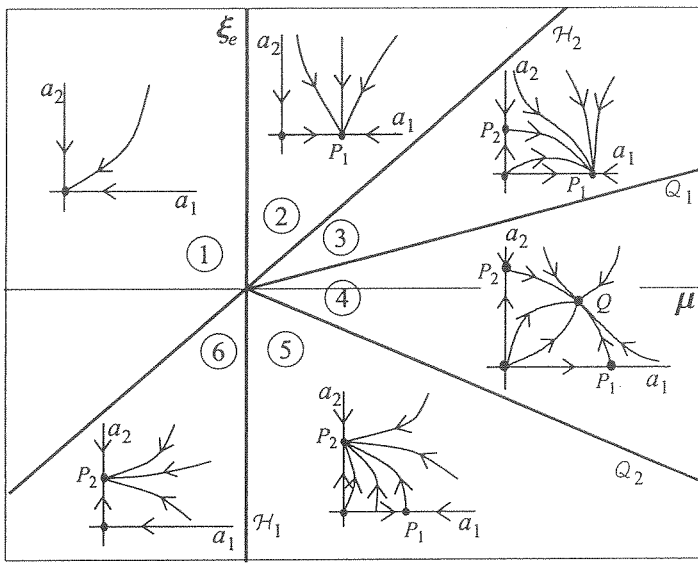


Figure 8. Bifurcation diagram for the nonresonant system in Fig. 2e; (a_1, a_2) amplitudes of the (antisymmetric, symmetric) mode.

lower ε^3 -order; they read:

$$\begin{aligned} \dot{A}_1 &= \mathcal{L}_1(\mu A_1, A_1^2 \bar{A}_1, A_1 A_2 \bar{A}_2, \bar{A}_1^2 A_2) \\ \dot{A}_2 &= \mathcal{L}_2(\mu A_2, A_2 A_1 \bar{A}_1, A_2^2 \bar{A}_2, A_1^3) \end{aligned} \quad (72)$$

which differ from Eq. (70), relevant to the nonresonant case, in their last terms, produced by the resonance (see also Eq. (45₂)).

In the 1:2 resonance, the quadratic nonlinearities $\mathbf{F}_{xx}^0 x_1^2$ produce resonant terms. It is therefore necessary to consider the complete expansion of d/dt and to perform the ordering $\mu = \varepsilon \hat{\mu}$. Solvability conditions are found both at the ε^2 -order and at the ε^3 -order; when these are reconstituted, the following bifurcation equations are finally obtained:

$$\begin{aligned} \dot{A}_1 &= \mathcal{L}_1(\mu A_1, \mu^2 A_1, A_2 \bar{A}_1, A_1^2 \bar{A}_1, A_1 A_2 \bar{A}_2) \\ \dot{A}_2 &= \mathcal{L}_2(\mu A_2, \mu^2 A_2, A_1^2, A_2 A_1 \bar{A}_1, A_2^2 \bar{A}_2) \end{aligned} \quad (73)$$

These can be considered as being derived from Eqs. (45₂) by putting $a_0 = 0$ and accounting for the quadratic combinations of the amplitudes producing resonances (note that cubic and, in general odd, combinations, only produce terms such as $A_i A_i \bar{A}_i$, also present in the nonresonant case).

By using a polar representation for the amplitudes, Eqs. (72) and (73) lead to a set of three differential equations in the real amplitudes a_1, a_2 and in the phase combination $\gamma := \vartheta_2 - n \vartheta_1$, with $n = \omega_2/\omega_1 = 2, 3$. The reduced bifurcation equations have the

following form when $n = 3$:

$$\begin{aligned} \dot{a}_1 &= \mathcal{R}_1(\boldsymbol{\mu}a_1, a_1^3, a_1a_2^2, a_1^2a_2 \exp(i\gamma)) \\ \dot{a}_2 &= \mathcal{R}_2(\boldsymbol{\mu}a_2, a_1^2a_2, a_2^3, a_1^3 \exp(-i\gamma)) \\ a_1a_2\dot{\gamma} &= a_1\mathcal{J}_2(\cdot) - 3a_2\mathcal{J}_1(\cdot) \end{aligned} \quad (74)$$

and the following form when $n = 2$:

$$\begin{aligned} \dot{a}_1 &= \mathcal{R}_1(\boldsymbol{\mu}a_1, \boldsymbol{\mu}^2a_1, a_1a_2 \exp(i\gamma), a_1^3, a_1a_2^2) \\ \dot{a}_2 &= \mathcal{R}_2(\boldsymbol{\mu}a_2, \boldsymbol{\mu}^2a_2, a_1^2 \exp(-i\gamma), a_2a_1^2, a_2^3) \\ a_1a_2\dot{\gamma} &= a_1\mathcal{J}_2(\cdot) - 2a_2\mathcal{J}_1(\cdot) \end{aligned} \quad (75)$$

where the arguments of \mathcal{J}_h , equal to that of \mathcal{R}_h , have been omitted.

In Ref. [25] an alternate mixed polar-Cartesian representation of the complex amplitudes has been adopted, namely: $A_1 = 1/2ae^{i\vartheta}$, $A_2 = 1/2(u+iv)e^{i\eta}$, leading to a set of *polynomial* (rather than transcendent) equations in the unknowns (a, u, v) . Such equations are in standard normal form, unlike Eqs. (74) and (75), and are therefore amenable to be analyzed by automatic tools such as AUTO [46].

As an example, the (nonlinear) resonant system in Fig. 2e has been extensively studied in Ref. [25]. A few results limited to the 1:3 resonance are illustrated here. The bifurcation scenario should be analyzed in the three-dimensional space of the bifurcation parameters $(\boldsymbol{\mu}, \kappa_e, \rho)$. Figures 9a, b are sections of this space for two values of the detuning parameter ρ ($\rho = 0$ denotes exactly tuned frequencies). In addition to the two Hopf boundaries \mathcal{H}_i of the linear stability analysis (see Fig. 6a), three other boundaries \mathcal{Q}_j are found, at which Neimark bifurcations take place, triggering quasi-periodic motions of the system. While the \mathcal{H}_i -boundaries are insensitive to the detuning parameter (as already observed in Sect. 3.5), the \mathcal{Q}_j -boundaries strongly depend on ρ . For a selected value of ρ (Fig. 9c) the bifurcation scenario is depicted on the $(\boldsymbol{\mu}, \kappa_e)$ -plane. The curves \mathcal{H}_i and \mathcal{Q}_j bound eight regions in which qualitatively different phase-portraits exist. These have been represented in the figure in the bidimensional state-space (a_1, a_2) , by ignoring the effects of the third state-variable γ ; in particular, the crossings of the projected trajectories are not shown and the flow is only sketched. Equilibrium points for the bifurcation equations (74) correspond to the periodic motion for the original system (in particular, $\dot{\gamma} = 0$ entails the nonlinear frequencies $\Omega_i = \omega_i + \vartheta_i$ remaining in integer ratio); moreover, limit-cycles for Eqs. (74) correspond to quasi-periodic solutions. These are denoted by P_i and q_j , respectively in Fig. 9c. By moving counterclockwise from region 1 to region 5, the following scenario is displayed: in region 1 the trivial solution is stable; in region 2, after a Hopf bifurcation at \mathcal{H}_1 , a stable periodic motion P_1 arises; in region 3, after the Neimark boundary \mathcal{Q}_1 is crossed, P_1 loses stability and a stable quasi-periodic solution q_1 is borne; in region 4 an unstable periodic motion P_2 arises; in region 5, the quasi-periodic motion disappears and P_1 regains stability. Moving clockwise

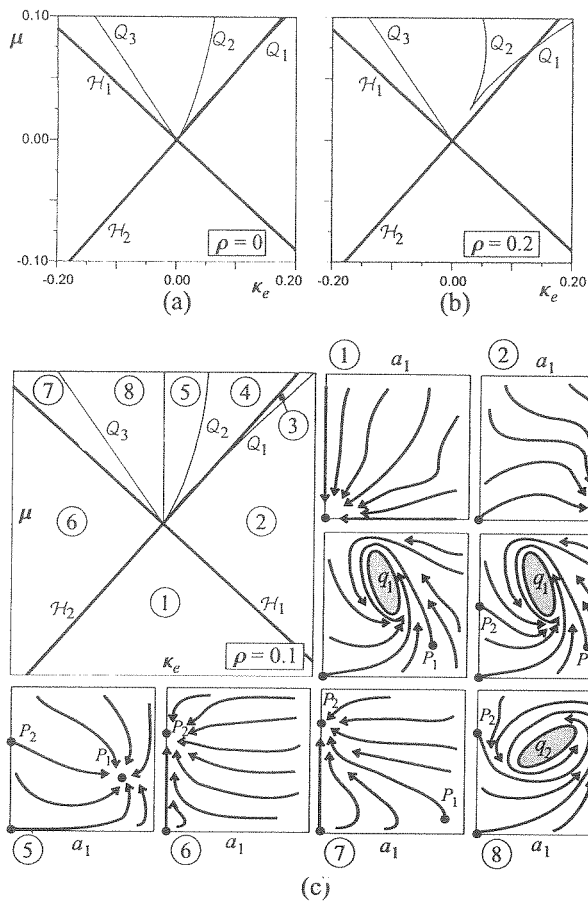


Figure 9. Bifurcation diagram for the 1:3 resonant system in Fig. 2e.

from region 6 to region 8: in region 6, after crossing the boundary \mathcal{H}_2 , the stable periodic motion P_2 is borne; in region 7, due to a second Hopf bifurcation occurring at \mathcal{H}_1 , an unstable motion P_1 appears; in region 8, a stable quasi-periodic solution q_2 arises, while P_2 loses stability. It should be noted that in each region there exists only one attractor, namely a periodic motion (in regions (1, 2, 5, 6, 7)) or a quasi-periodic motion (in regions 3, 4, 8).

7.4. Double-zero bifurcation

The motion is described, at the leading order, by Eq. (51). Since the bifurcation is defective, series of powers of $\varepsilon^{1/2}$ must be employed for both \mathbf{x} and d/dt (Eq. (48)); $\boldsymbol{\mu} = \varepsilon \hat{\boldsymbol{\mu}}$ must also be posed, with $\boldsymbol{\mu} \in \mathbb{R}^2$. Solvability conditions at the orders

ε^2 , $\varepsilon^{5/2}$, ε^3 and $\varepsilon^{7/2}$ are enforced and, after reconstitution, lead to the following bifurcation equation:

$$\ddot{a} = \mathcal{L}(\boldsymbol{\mu}a, a^2; \boldsymbol{\mu}\dot{a}, a\dot{a}; \boldsymbol{\mu}^2a, a^3, \dot{a}^2, \boldsymbol{\mu}a^2; \boldsymbol{\mu}a\dot{a}, \boldsymbol{\mu}^2\dot{a}, a^2\dot{a}) \quad (76)$$

By remembering that $a = O(\varepsilon)$, $\boldsymbol{\mu} = O(\varepsilon)$ and $d/dt = O(\varepsilon^{1/2})$, the right hand member of Eq. (76) contains all the terms of the order ε^2 , $\varepsilon^{5/2}$, ε^3 and $\varepsilon^{7/2}$. It is interesting to observe that the MSM leads directly to a bifurcation-equation in the (more convenient) Bogdanova-Arnold normal form, in contrast to the Center Manifold Method, where the final form depends on some arbitrary choices.

Equation (76) has been used in [21] to analyze the double-zero bifurcation of a nonlinear two d.o.f. system, depending on two bifurcation parameters $\boldsymbol{\mu} = (\kappa, \xi)$, exhibiting a behavior similar to that of the single d.o.f. system in Fig. 2c. In contrast to this, however, the linear terms in \dot{a} and a in Eq. (76) depend nonlinearly on $\boldsymbol{\mu}$; this means that the Hopf- and divergence-boundaries \mathcal{H}_T and \mathcal{D} (at which the trivial solution $\mathbf{x} = \mathbf{0}$ loses stability) are curves tangent to the κ - and ξ -axes, respectively, rather than straight lines (Fig. 10 should be compared with Fig. 3). Along the divergence boundary a transcritical bifurcation takes place, from which a non-trivial solution emerges. This loses stability at the boundary \mathcal{H}_{NT} , where a new Hopf bifurcation manifests itself. Moreover, two further curves \mathcal{N}_T and \mathcal{N}_{NT} organize the parameter plane, being loci of systems having two coincident eigenvalues. Finally, two dashed lines are indicated, along which there is a collision between a limit-cycle and a saddle-point (homoclinic bifurcation). To sum up, Fig. 10 describes the following scenario, going from region 1 to 5 or, similarly, from region 6 to 10: first the equilibrium points are a stable node and a saddle; the node then modifies to become a focus; after a Hopf bifurcation, the focus becomes unstable and a limit cycle p arises; after colliding with the saddle, the limit cycle disappears; finally, the focus becomes an unstable node.

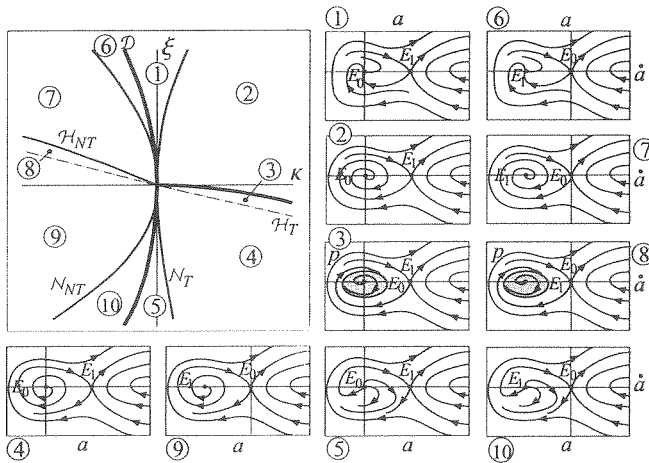


Fig. 10. Bifurcation diagram for a system exhibiting a double divergence.

7.5. 1:1 Resonant double-Hopf bifurcation

The motion is described, at the leading order, by Eq. (59). Since the bifurcation is defective and the multiplicity $m = 2$ is even, series (48) must be employed retaining only the even powers of $\varepsilon^{1/2}$; the parameters $\mu \in \mathbb{R}^3$ must also be ordered as $\mu = \varepsilon^2 \bar{\mu}$. When the solvability conditions at the ε^3 - and ε^4 -orders have been reconstituted, they furnish the following bifurcation equation:

$$\ddot{A} = \mathcal{L}_0(\mu A, A^2 \bar{A}) + \mathcal{L}_1(\mu \dot{A}, A \bar{A} \dot{A}, A^2 \bar{\dot{A}}) \quad (77)$$

By remembering that $A = O(\varepsilon)$, $\mu = O(\varepsilon^2)$ and $d/dt = O(\varepsilon)$, the right member of Eq. (77) contains all the resonant terms of orders ε^3 and ε^4 . Equation (77) is a second-order differential equation in the complex amplitude A ; by adopting the polar representation $A = 1/2 a e^{i\vartheta}$ and recasting the equations in state-variable form, three first order equations are drawn, namely:

$$\begin{aligned} \dot{a} &= r \\ \dot{r} &= as^2 + \mathcal{R}_0(\mu a, a^3) + \mathcal{R}_1(\mu r, a^2 r, a^2 r) - \mathcal{F}_1(\mu as, a^3 s, -a^3 s) \\ \dot{a}s &= -2rs + \mathcal{F}_0(\mu a, a^3) + \mathcal{F}_1(\mu r, a^2 r, a^2 r) - \mathcal{R}_1(\mu as, a^3 s, -a^3 s) \end{aligned} \quad (78)$$

uncoupled from the fourth $\dot{\vartheta} = s$. Equations (78) govern the behavior of the system around the codimension-3 bifurcation. Steady-state solutions to Eqs. (78) are periodic motions for the original system of amplitude $a = \text{const}$ and nonlinear frequency $\Omega = \omega + s$. Since a cubic equation in a^2 can be drawn from the steady version of Eqs. (78), from zero to three periodic motions can co-exist in the neighborhood of the bifurcation point.

Equations (78) are used in Ref. [26] to analyze the post-critical behavior of the 1:1 resonant system in Fig. 2e and in Ref. [27] to study the effectiveness of Tuned Mass Dampers in the nonlinear passive control of aerolastic oscillators. With reference to the first problem, Fig. 11a shows a section of the space of the bifurcation parameters (Fig. 6b)

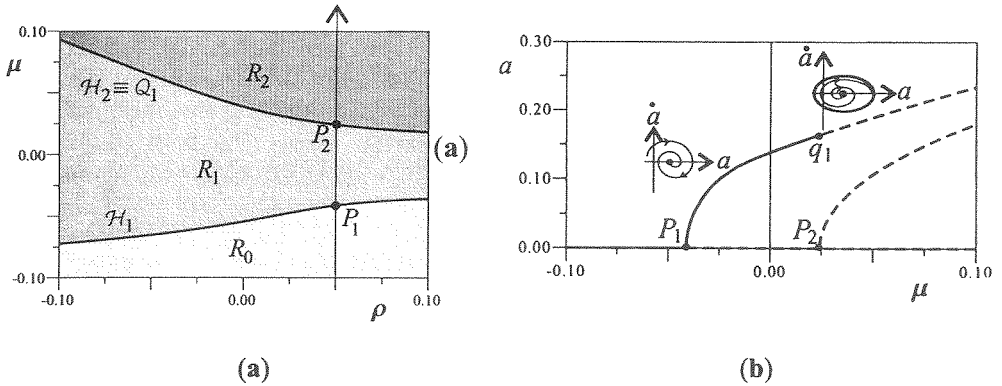


Figure 11. (a) Bifurcation diagram and (b) fixed points bifurcation diagram for the 1:1 resonant system in Fig. 2e.

for $\kappa_e = \text{const.}$ At the boundaries \mathcal{H}_1 and \mathcal{H}_2 the trivial solution undergoes Hopf bifurcations. If ρ is also kept constant and the wind velocity μ is increased along the path shown in Fig. 11a, the bifurcation diagram of Fig. 11b is obtained. The amplitude of the stable limit cycle bifurcating from the trivial solution at \mathcal{H}_1 increases until the boundary \mathcal{H}_2 is reached. There a second, unstable, limit cycle bifurcates from the trivial solution, while the first limit cycle also becomes unstable and a quasi-periodic solution bifurcates from it. There thus exist only the trivial solution in R_0 , one stable periodic motion in R_1 and two unstable periodic motions in R_2 , in addition to the stable quasi-periodic motion. Moreover, \mathcal{H}_2 is both a Hopf boundary for the trivial solution and a Neimark boundary \mathcal{Q}_1 for the limit cycle bifurcating at \mathcal{H}_1 .

8. Conclusion

We have analyzed codimension- M bifurcations for finite- dimensional autonomous systems. The following conclusions are drawn.

- (1) A bifurcation from equilibrium points occurs in autonomous systems when, by varying the control parameters, several eigenvalues of the Jacobian matrix simultaneously cross the imaginary axis of the complex plane. The number of the critical eigenvalues (real or complex, with the latter counted in pairs) plus the number of the resonance conditions among their imaginary parts, is called *the (linear) codimension M of the bifurcation*.
- (2) A (perfect) bifurcation requires at least M parameters to occur as a generic (structurally stable) case. Imperfection parameters can also be accounted for as parameters that destroy the fundamental path and produce non-zero effects in the critical eigenspace.
- (3) Sample mechanical systems with one or two d.o.f. reveals all the aspects of the (linear) bifurcation mechanisms of low-codimension. Thus, the stiffness and the damping of a single d.o.f. system are responsible for divergence and Hopf bifurcations, respectively. If they occur simultaneously, they lead either to the double-zero bifurcation or to the Hopf-divergence bifurcation. In the former case, the Hopf boundary dies at the crossing with the divergence boundary whereas in the latter case the two manifolds cross each other. The double-zero bifurcation reveals the existence of a family of (non critical) nilpotent systems, to which the bifurcation point belongs and which organizes the linear stability diagram. Non- generic double-zero bifurcations have also been discussed, leading to simultaneous multiple divergences. By referring to a simple model, double-Hopf bifurcations, both of a nonresonant ($M=2$) or a resonant ($M=3$) type have been analyzed. The mechanism leading to non-defective (1:2, 1:3,...) or defective (1:1) resonant bifurcations has been illustrated.
- (4) Eigenvalues sensitivity analysis has been studied. Apart from its intrinsic value, this also suggests strategies for solving nonlinear bifurcation problems, particularly in defective cases. Integer power series expansions of the perturbation parameters must be used for non-defective critical eigenvalues, while fractional power series expansions must be employed for defective eigenvalues. Most importantly, since the fractional series become singular for special perturbations (which are always encountered if the whole neighborhood

of the bifurcation point has to be spanned), it is convenient to resort to a *reconstituted eigenvalue sensitivity equation*, valid for any perturbation. This equation is of a *degree equal to the algebraic multiplicity of the defective eigenvalue*.

- (5) Multiple Scale Analysis for *non-defective* bifurcations requires the use of integer power expansions for both the state variables and the time-derivatives. By accounting for the possible resonance conditions among the critical frequencies, solvability conditions are enforced at each step of the perturbation procedure. These furnish a set of complex equations governing the amplitude evolution on a single time-scale. Rules to build up the structure (i.e., to within the complex coefficients) of such equations to the desired order have been given.
- (6) Some algorithmic aspects of Multiple Scale Analysis have been illustrated, concerning: (a) the convenience of expanding or simply ordering the bifurcation parameters; (b) the search for a steady solution, requiring the availability of a number of parameters equal to that of the codimension of the bifurcation, thus confirming from an algorithmic point of view the need for such coincidence; (c) the reconstitution procedure, similar to that used in Sensitivity Analysis, furnishing bifurcation equations on the true time-scale; (d) the possibility to account for imperfection parameters.
- (7) Multiple Scale Analysis for *defective* bifurcations in which just one $m \times m$ Jordan block is associated with the critical eigenvalue, has also been illustrated. Fractional power series expansions of both the state variables and the time-derivative must be employed, namely: (a) *complete* series of powers of $\varepsilon^{1/m}$ for the defective divergence; (b) series of *even* powers of $\varepsilon^{1/m}$ for defective Hopf bifurcations when m is *even*; (c) *complete* series of powers of $\varepsilon^{1/m}$ for the state variables and series of *even* powers of $\varepsilon^{1/m}$ for the time-derivative when m is *odd*. In all cases the same rule holds: *the reconstituted bifurcation equation is an m -th order differential equation containing all resonant terms products of the parameters, of the amplitude and its derivatives; all terms are of an order of magnitude between that of the m -th derivative and the highest perturbation order accounted for in the analysis*.
- (8) The techniques illustrated have been applied to several problems of codimension-2 or -3. The post-critical behavior of the sample structures introduced before has been briefly commented in the bifurcation parameter space and, in one case, the effect of the imperfections has been accounted for.

Acknowledgement

This work was partially supported by the 'Italian Ministry of Universities and Scientific Research', under the projects PRIN 1997/98, 1999/00 and 2001/02.

References

1. Arnold, V.I., Geometrical Methods in the Theory of Ordinary Differential Equations, Springer Verlag, New York, Heidelberg, Berlin, 1982. (Russian original, Moscow, 1977).
2. Guckenheimer, J., and Holmes, P., Nonlinear Oscillations, Dynamical Systems, and Bifurcations of Vector Fields, Springer-Verlag, New York, 1983.

3. Troger, H., and Steindl, A., *Nonlinear Stability and Bifurcation Theory*, Springer Verlag, Wien, New York, 1991.
4. Wiggins, P., *Global Bifurcations and Chaos*, Springer Verlag, , 1988.
5. Sewell, M. J., 'A General Theory of Equilibrium Paths Trough Critical Points. I,II' *Proc. Roy. Soc.*, 1968.
6. Sewell, M. J., 'On the Branching of Equilibrium Paths', *Proc. Roy. Soc.*, 1970.
7. Thompson, J.M.T., and Hunt, G.W., *A General Theory of Elastic Stability*, Wiley, London, 1973.
8. Pignataro, M., Rizzi, N., and Luongo, A., *Stability, Bifurcation, and Postcritical Behavior of Elastic Systems*, Elsevier, Amsterdam, 1991. (Italian original, Rome, 1983).
9. Friedman, B., *Principies and Techniques of Applied Mathematics*, John Wiley, New York, 1956.
10. Nayfeh, A.H., *Introduction to Perturbation Techniques*, Wiley-Interscience, New York, 1991.
11. Nayfeh, A.H., 'Nonlinear Stability of a Liquid Jet', *Physics of Fluids* **13**, 1970, 841-847.
12. Smith, L.L., and Morino, L., 'Stability Analysis of Nonlinear Differential Autonomous Systems with Applications to Flutter', *AIAA Journal* **14**, 1976, 333-341.
13. Nayfeh, A.H., and Balachandran, B., *Applied Nonlinear Dynamics*, Wiley-Interscience, New York, 1995.
14. Paolone, A., *Asymptotic Methods for Stability and Bifurcation Analysis of Non-Conservative Nonlinear Mechanical Systems*, Ph.D. Thesis, University of Rome "La Sapienza" (in Italian), 1995.
15. Luongo, A., and Di Fabio, F., 'Multimodal Galloping of Dense Spectra Structures', *J. Wind Eng.Ind.Aerodynamics*, (48), 1993, 163-174.
16. Luongo, A., 'Perturbation Methods for Nonlinear Autonomous Discrete-Time Dynamical Systems', *Nonlinear Dynamics* **10**, 1996, 317-331.
17. Luongo, A., and Paolone, A., 'Perturbation Methods for Bifurcation Analysis from Multiple Nonresonant Complex Eigenvalues', *Nonlinear Dynamics*, **14**, 1997, 193-210.
18. Luongo, A., and Piccardo, G., 'Non-Linear Galloping of Saggged Cables in 1:2 Internal Resonance', *Journal of Sound and Vibration*, **214**(5), 1998, 915-940.
19. Luongo, A., Paolone, A., and Piccardo, G., 'Postcritical Behavior of Cables Undergoing Two Simultaneous Galloping Modes', *Meccanica*, **33**, 1998, 229-242.
20. Luongo, A., and Paolone, A., 'Multiple Scale Analysis for Divergence-Hopf Bifurcation of Imperfect Symmetric Systems', *Journal Sound and Vibration*, **218**, 1998, 527-539.
21. Luongo, A., Paolone A., and Di Egidio, A., 'Multiple Time Scale Analysis for Bifurcation from a Double-Zero Eigenvalue', 1999 *ASME*, Las Vegas, Nevada.
22. Gattulli, V., Di Fabio, F, and Luongo, A., 'Simple and Double Hopf Bifurcations in aerolastic Oscillators with Tuned Mass Dampers', *Journal of Franklin Institute*, **338**(2, 3), 2001, 187-201.
23. Natsiavas, S., 'Free Vibration of Two Coupled Nonlinear Oscillators', *Nonlinear Dynamics*, **6**, 1994, 69-86.
24. Natsiavas, S., 'Free Vibration in a Class of Self-Excited Oscillators with 1:3 Internal Resonance', *Nonlinear Dynamics*, **12**, 1997, 109-128.
25. Luongo, A., Paolone, A., and Di Egidio, A., 'Multiple Time Scales Analysis for 1:2 and 1:3 Resonant Hopf Bifurcations', 2001, *Nonlinear Dynamics*, submitted.
26. Di Egidio, A., Paolone, A., and Luongo, A., 'Post-Critical Analysis of Self-Excited Structures in 1:1 Resonance Condition', *Proc. of the XIV Italian Congress of Theoretical and Applied Mechanics*, 1999, Como, Italy (in Italian).
27. Gattulli, V., Di Fabio, F., and Luongo, A., 'Effects of tuned mass dampers on aeroelastic oscillators', *Journal of Sound and Vibration*, 2001, submitted.
28. Iooss, G., and Joseph, D.D., *Elementary Stability and Bifurcation Theory*, Springer-Verlag, New York, 1980.
29. Blevins, R.D., *Flow induced vibration* (second edition), Van Nostrand Reinhold, New York, 1990.
30. Luongo, A., Paolone, A., and Di Egidio, A., 'Sensitivities and Linear Stability Analysis Around a Double Zero Eigenvalue', *AIAA Journal*, **38**(4), 2000, 702-710.
31. Potier-Ferry, M., 'Foundation of Elastic Postbuckling Theory', in *Buckling and postbuckling*, Four lectures in experimental, numerical and theoretical solid mechanics, CISM-Meeting, Italy, September 29-October 3, Springer-Verlag, 1985.
32. Budiansky, B., 'Theory of Buckling and Post-Buckling Behaviour of Elastic Structures', *Advanced*

- in *Applied Mechanics*, **14**, Chia-Shun Yih (ed), New York, Academic Press, 1974, 1-65.
33. Byskov, E., and Hutchinson, J.W., 'Mode Interaction in Axially Stiffened Cylindrical Shells', *AIAA Journal*, **15**(7), 1977, 941-948.
 34. Gioncu, V., "General theory of coupled instabilities", *Thin Walled Structures*, **19**, 1994, 81-127.
 35. Pignataro, M., and Luongo, A., 'Interactive Buckling of an Elastically Restrained Truss Structure', *Thin Walled Structures*, **19**, 1994, 197-210.
 36. Augusti, G., Some Problems in Structural Instability, with Special Reference to Beam-Columns of I-Section, Part I: Investigations on the Basic Types of Elastic Buckling and Post-Buckling by Means of Semi-Rigid Models, Ph.D. Thesis; University of Cambridge, Department of Engineering, 1964.
 37. Leipholz, H., Stability of Elastic Systems, Sijthoff and Noordhoff, The Netherlands, 1980.
 38. Bowen, R.M., and Wang, C.C., Introduction to Vectors and Tensors – Part A: Linear and Multilinear Algebra, Plenum Press, New York, 1980.
 39. Wilkinson, J.H., The Algebraic Eigenvalue Problem, Clarendon Press, Oxford, England, UK, 1965.
 40. Luongo, A., 'Eigensolutions Sensitivity for Nonsymmetric Matrices with Repeated Eigenvalues', *AIAA Journal*, **31**, 1993, 1321-1328.
 41. Paolone A., Di Egidio A., and Luongo A. 'A Reduction Method for Spectral Sensitivity Analysis of Linear Mechanical Systems', Proc. of the XIV Italian Congress of Theoretical and Applied Mechanics, 1999, Como, Italy, (in Italian).
 42. Luongo, A., Paolone, A., and Di Egidio, A., 'Classes of Motion Qualitative Analysis for Multiresonant Systems: I An Algebraic Method. II A Geometrical Method', submitted.
 43. Luongo, A., Di Egidio, A., and Paolone, A., 'On the Proper Form of the Amplitude Modulation Equations for Resonant System", 2001, *Nonlinear Dynamics*, in press.
 44. Nayfeh, A.H., 'Topical Course on Nonlinear Dynamics', Società Italiana di Fisica, Santa Margherita di Pula, Sardinia, Perturbation Methods in Nonlinear Dynamics, 1985.
 45. Luongo, A. and Paolone A., 'On the Reconstitution Problem in the Multiple Time Scale Method", *Nonlinear Dynamics*, **14**, 1999, 133-156.
 46. Doedel, E., and Kernevez, J.P., 'AUTO: Software for Continuation and Bifurcations Problem in Ordinary Differential Equations", Applied Math. Report, California Institute of Technology, 1986.